

## LIST OF SUPPLEMENTARY MATERIALS

Methods

Methods references

Supplementary Tables (4 supplementary tables)

Supplementary Figures plus Legends (17 supplementary figures)

## METHODS

See Tables 1, 2 and 3 for strains, plasmids and oligonucleotides used in this study.

### Growth conditions

*General growth conditions* - Cultures of *S. aureus* or *E. coli* were grown according to the following generic growth protocol unless otherwise indicated. The preparation of the inoculum consisted on growth of an initial pre-inoculum of the selected strain in Brain Heart Infusion broth (BHI; Oxoid) overnight that had been inoculated from a fresh isolate on plates of solid BHI medium (BHI-A). The pre-inoculum was subsequently subcultured into BHI broth to a final OD<sub>600</sub>~ 0.01 and grown to mid-exponential phase (OD<sub>600</sub>~ 0.4-0.6) to produce the inoculum for the assay cultures; the latter were inoculated to a final OD<sub>600</sub>~ 0.01. On studies of MreCD function Luria Bertani broth (LB; from Oxoid, England) was used instead of BHI for the pre-inoculum and inoculum cultures. Other growth media used in this work were, Tryptone Soy Broth (TSB) and LK (1). Growth was undertaken at 37°C, unless otherwise stated, and growth in liquid media was carried out in an orbital shaker at 250rpm. For growth on solid media 1.5% (w/v) agar was added to the liquid medium resulting in BHI-A, TSB-A, LB-A, or LK-A plates. When required supplements were added to pre-inoculum, inoculum, and assay cultures. The antibiotics used were: ampicillin (Amp, 100µg ml<sup>-1</sup>), chloramphenicol (Cat, 30µg ml<sup>-1</sup>), tetracycline (Tet, 10µg ml<sup>-1</sup>), erythromycin (Ery, 5µg ml<sup>-1</sup>), kanamycin (Kan, 50 µg ml<sup>-1</sup>), neomycin (Neo, 50µg ml<sup>-1</sup>) and lincomycin (Lin, 25µg ml<sup>-1</sup>). Selection of *S. aureus* strains containing the *ery* or *kan* genes was made on Ery/Lin and Kan/Neo, respectively.

*Depletion studies* - The JGL166 pre-inoculum was grown in the presence of 20µM IPTG and 30µg/ml Cat to an OD<sub>600</sub>~0.3, washed with fresh BHI (at 37°C) and re-subcultured to an OD<sub>600</sub>~ 0.0001 (for essentiality studies) or 0.1 (for microscopy studies) in the presence (20µM) or absence of IPTG. Ideal concentrations for depletion were obtained from equivalent preliminary studies using a range of IPTG concentrations (from 0 to 500µM). Growth was determined by absorbance (OD<sub>600</sub>) and viable counts (colony forming units / ml, CFU/ml).

### Strain and plasmid constructions

Transformations of *S. aureus* strain RN4220 were performed as described by Schenk and Laddaga (2). All phage transductions were performed using Φ11 as described previously (1). DNA manipulation and *E. coli* transformations were performed

according to the method of Sambrook and Russell (3). Genetic constructions were generated by either conventional enzymatic restriction and ligation of inserts into vectors (typically using electrocompetent *E. coli* TOP10 as a primary recipient), or by *in vivo* genetic engineering using Lambda Red-mediated recombination of PCR amplified inserts into selected vectors (4) with specially designed oligonucleotide primers and recombination-induced electrocompetent *E. coli* EL250 cells (4). The restriction deficient *S. aureus* strain RN4220 was used as an intermediate passage strain for plasmids to be transferred into other *S. aureus* strains unless otherwise indicated (5).

*Construction of a temperature sensitive ori plasmid vector* - The 338bp MCS from pSL1190 was produced by PCR (oligonucleotide primers 5'GLUSh66a/3'GLUSh66a) and inserted by Lambda Red into pAZ106 replacing a 3621bp fragment including *lacZ*, and generating plasmid pGL456. At the BstBI site of pGL456 was cloned the temperature sensitive *S. aureus* origin of replication pE194<sup>ts</sup> flanked by ClaI sites in pLL2443, resulting in plasmid pGL471b.

*Construction of a strain enabling exogenous control of *plsY* expression* - A region of 3922bp from the chromosome of *S. aureus* SH1000 centered in *plsY* was PCR amplified (oligonucleotides 5'GLUSh3K/3'GLUSh3K) and Lambda Red inserted into pOB, resulting in plasmid pGL401. The Tet-T-P<sub>spac</sub> cassette from plasmid pGL400 (6) was amplified (oligonucleotides 5'GLUSh16c and 3'GLUSh16c) and placed upstream of *plsY* in pGL401 through Lambda Red recombination generating plasmid pGL412. pGL471b was used as a backbone to receive at its BamHI site the Tet-T-P<sub>spac</sub>~*plsY* fragment surrounded by the chromosomal *plsY* region in pGL412, which was PCR amplified (oligonucleotide primers 5'GLUSh3F/3'GLUSh3F). The resulting plasmid - pGL484- was electroporated into strain RN4220 (generating strain JGL145) and from there it was transduced into SH1000 at the permissive temperature (30°C) (7). SH1000 pGL484-containing transductants were selected by resistance to Tet and Ery on LK-A plates at 30°C. The generation of double cross-over recombinants where the native P<sub>plsY</sub>~*plsY* of SH1000 had been replaced by the Tet-T-P<sub>spac</sub>~*plsY* fragment through its flanking fragments with homology to the chromosomal *plsY* region was triggered by exposing single colonies from several of the freshly streaked isolates growing at the permissive temperature to 3 consecutive cycles of re-streaking and overnight (O/N) growth at 42°C (restrictive temperature). Each colony was streaked on two independent plates of BHI-A Tet (5µg/ml) incubated at 30°C and 42°C O/N, respectively. Streaks showing poor growth on the 42°C plates and inability to grow on BHI-A Ery/Lin plates were chosen as candidates and used as recipients of plasmid pGL485 by transduction selecting on LK-A Cat 500µM IPTG. The resulting strain was grown in 5ml of BHI Cat 500µM IPTG until mid-exponential, and then subcultured in BHI Cat 200µM IPTG. The latter was the inoculum of BHI containing 500 or 0µM IPTG; from there was isolated strain JGL166 (JGL153/pGL485). The correct genetic constructs were confirmed by PCR and DNA sequencing.

*Construction of GFP reporter fusions* – Plasmid pGL503 was generated through the insertion into pMUTIN~GFP+ of an approx. 750bp DNA fragment containing the entire *plsY* gene that was PCR amplified (oligonucleotide primers 5'GLUSh190A/3'GLUSh190A) from a SH1000 genomic DNA template. The cloning was carried out at the KpnI/EagI sites and was made in frame with the *gfp+* gene. Equivalent reporter fusions of the MreC (pGL516), MreD (pGL517) and SecY (pGL519) proteins from *S. aureus* to GFP were made through PCR amplification of the corresponding gene sequences and subsequent cloning into the KpnI/EagI sites of pGL503 thus removing the *plsY* insert. These plasmids were electroporated into *S. aureus* RN4220. Plasmid integration via a single-cross-over event at the chromosomal locus of *plsY*, *mreC*, *mreD* or *secY* resulted in an intact copy of the corresponding gene under the control of P<sub>spac</sub> and a fusion of the gene of interest to *gfp+* under the control of the native promoter of the corresponding gene. The resulting RN4220-based strains were named as JGL219, JGL223, JGL224, and JGL225, respectively. The GFP fusions were subsequently transduced into a SH1000 giving rise to strains JGL232, JGL229, JGL230 and JGL231, respectively. In addition, a PBP2~GFP transcriptional fusion from RNpBP2-31 was transduced into strain JGL166 giving rise to strain JGL241.

*Construction of deletion strains* – For the construction of the MreD deficient strain the following steps were undertaken. DNA fragments for 2.2kb upstream including *mreC* gene and 1kb downstream sequences of *mreD* were PCR amplified from *S. aureus* SH1000 chromosomal DNA (oligonucleotide primers: 5'GLUSh270A/3'GLUSh270D for the upstream fragment and 3'GLUSh270C/3'GLUSh270A for the downstream fragment). The resulting fragments were digested with BamHI/NotI and KpnI/NotI, respectively, and were ligated into the corresponding sites of pOB to generate pGL589. A 1.5kb Kan resistance cassette from pGL433 was generated by PCR (oligonucleotide primers 5'HXM39B/3'HXM39B) and cloned into NotI site between the upstream and downstream sequences rendering pGL607a. A PCR amplified fragment from the resulting construct (oligonucleotide primers 5'GLUSh270A/3'HXM67A) was cloned at the BamHI/BglII sites of pMAD resulting in plasmid pGL613, which was used to transform *S. aureus* RN4220. A pMAD-based allelic replacement in *S. aureus*, was favoured through a temperature shift from 30°C to 42°C (8), and it was transferred into SH1000 by transduction. The correct double-cross-over chromosomal exchange was verified by southern blot.

An unmarked in frame *mreC* deletion mutant was constructed using plasmid pXIM5, a pIMAY (9) derivative containing regions upstream (oligonucleotide primers 5HXM292/5GLUSh270C; 1289 bp) and downstream (5GLUSh270D/3GLUSh270A; 1570 bp) of the *S. aureus mreC* gene. The upstream arm carries the native promoter of the *mreC* gene; the downstream arm encodes residues 807-843 of *mreC*, corresponding to the extreme C terminus of MreC subdomain, which carries the ribosome binding site of *mreD* gene and the entire *mreD* gene. These regions were PCR amplified from *S. aureus* SH1000 genomic DNA, digested with NotI/SacI and NotI/KpnI, respectively. The purified fragments were mixed with a SacI/KpnI

digested and alkaline phosphatase dephosphorylated pIMAY in a three-way ligation reaction to generate pXIM5 in *E. coli* TOP10 after LB 15 µg ml<sup>-1</sup> Cat (37°C) selection. Following an intermediate *E. coli* DH10B passage, pXIM5 was electroporated into *S. aureus* RN4220 and pXIM5-containing transformants were selected on TSB Cat at 28°C. Integration of pXIM5 into the chromosome was achieved by successive plating of the resulting strain (SJF4057) at the non-replicating temperature of 39°C on TSB Cat. To select isolates that have lost the integrated plasmid and potentially excised *mreC*, pXIM5-containing isolates were grown on BHI agar plates in the presence of 1 µg ml<sup>-1</sup> anhydrotetracycline (ATc) for 5x O/N at 28°C. A  $\Delta mreC$  mutant (SJF4098) was confirmed by PCR (oligonucleotide primers 5'GLUSh270B/3'GLUSh270D and 5'GLUSh270B/3'GLUSh270B) and further verified by southern blot.

Construction of an *mreCD* deletion strain was achieved through allelic replacement of the region with a Kan<sup>R</sup> cassette through suicidal recombination. DNA fragments corresponding to the upstream and downstream regions of *mreCD* were PCR amplified from a *S. aureus* SH1000 DNA template (oligonucleotide primers 5'GLUSh270A/5'GLUSh270C and 3'GLUSh270C/3'GLUSh270A). Both DNA fragments were joined together at the NotI site and the resulting fragment cloned at the BamHI/KpnI sites of pOB generating plasmid pGL590. The Kan<sup>R</sup> cassette was obtained from pGL433b (PCR amplification using 5'HXM39B/3'HXM39B) and inserted at the NotI site of pGL590 generating pGL598b. The latter was electroporated into RN4220 where successful recombinants were selected by resistance to Kan and sensitivity to Ery/Lin. From there the deletion was transduced into SH1000 generating strain s2625. The absence of *mreC* and *mreD* were confirmed by PCR (oligonucleotide primers 5'GLUSh270A/3'GLUSh270D, 5'GLUSh270D/3'GLUSh270A, 5'/3'GLUSh270B and 5'GLUSh27B/3'GLUSh27B) and subsequently by Southern blot.

*Constructs to evaluate gene complementation* – Strain JGL232 upon transduction with pGL485 became strain JGL260, and was used for complementation studies to demonstrate that the PlsY~GFP fusion was functional. Complementation of the  $\Delta mreD$  mutant strain (SJF2976) was achieved through the ectopic insertion in the lipase gene of a chromosomal single-copy of *mreD* under the control of *mreCD* native promoter. The latter as well as the *mreD* gene were amplified from a wild type chromosomal DNA template using the primer pairs 5'FW94/3'FW94 and 5'FW95/3'FW93, respectively. Both fragments were cloned into the *Bam*HI/*Eco*RI site of pCL25 using Gibson Assembly (New England Biolabs, Hitchin, United Kingdom). pCL25 is a non-replicating plasmid in *S. aureus* and integrates into the lipase gene via site-specific recombination with help of an integrase encoded from plasmid pYL112 $\Delta$ 19 (10). The resulting plasmid pCL25-*mreD* was electroporated into RN4220 and subsequently transduced into SJF2976 and SH1000 generating strains SJF4650 and SJF4651, respectively.

*Constructs of BACTH plasmids and strains* – The coding sequences of *S. aureus* PlsY, CdsA, and MreD were cloned at the *Eco*RI/*Bam*HI sites of pKT25 (pGL555, pGL633,



pALB7, respectively). PlsY and MreD were also cloned into pUT18C (pGL568 and pALB11), while *cdsA* was cloned into pUT18 (pGL635).

*Constructs of FRET plasmids and strains* – The plasmid pWhiteWalker1 was constructed as follows: codon-optimized forms of the genes *mCherry* (Uniprot X5DSL3-1) and *gfp* (eGFP; Uniprot Q8GHE2-1) containing their own ribosomal binding sites were separately amplified by PCR (oligonucleotide primers: 5'FL04/3'pWhiteWalker0mCherryOE and 5' pWhiteWalker0GFPOE/3'FL05, respectively), fused by overlap extension PCR and cloned at the EcoRI/Ascl site of shuttle-vector pWhiteWalker0. A translational fusion of *mCherry-gfp* linked by a sequence encoding a Serine/Glycine linker was constructed by PCR amplification of *mCherry* and *gfp* (oligonucleotide primers: 5'FL04/3'FL04OE and 5'FL05OE/3'FL05, respectively), fusion of the fragments using overlap extension PCR and cloning of the final fragment at the EcoRI/Ascl site of pWhiteWalker0. This resulted in plasmid pWhiteWalker2. Construction of pWhiteWalker3 was carried out by amplification and cloning the gene coding for *S. aureus* PlsY (5'FL06/3'FL06) at the BglII/KpnI site of pWhiteWalker1 in lieu of *gfp*. Thus, resulting in an in-frame fusion of *plsY-gfp* and separate non-fused *mCherry*. pWhiteWalker 4 was then subsequently constructed from pWhiteWalker3. Firstly, a tandem fusion of *mreD* (5'FL07/3'FL07OE) and *mCherry* (5'FL08OE/3'FL04) was created by overlap extension PCR. This fragment contained flanking BglII and EcoRI sites as well as a ribosome-binding site. This was cloned into pWhiteWalker3 by an EcoRI/BglII digest to generate the final pWhiteWalker3 containing tandem fusions of *mreD-mCherry* and *plsY-gfp*. pWhiteWalker 5 was constructed from pWhiteWalker3 in the same manner as for pWhiteWalker4 (see above), using a gene encoding *cdsA* (5'FL09/3'FL09OE) fused by overlap extension PCR to *mCherry* (5'FL10OE/3'FL04) in lieu of *mreD*. The resulting construct contained tandem fusions of *cdsA-mCherry* and *plsY-gfp*. Plasmids pWhiteWalker10, 12 and 13 were constructed using Gibson Assembly (New England Biolabs, Hitchin, United Kingdom). pWhiteWalker3 was used as a template to amplify a tandem fusion of *plsY-gfp* (5'FW73/3'FW73) that was subsequently cloned into the *EcoRI/Ascl* sites of pWhiteWalker0 resulting in pWhiteWalker10. This plasmid expresses a tandem fusion of *plsY* and *gfp*, and was used as a negative control to calculate FRET efficiencies. In order to construct pWhiteWalker12 and 13, genes encoding *secY* and *mscL* were amplified from a SH1000 chromosomal DNA template using primer pairs 5'FW75/3'FW75 and 5'FW76/3'FW76, respectively. These DNA fragments were cloned by Gibson Assembly into a pWhiteWalker3 that had been digested with NheI and EcoRI to remove *mreD*. This resulted in plasmids containing tandem fusions of *secY-mCherry* (pWhiteWalker12) or *mscL-mCherry* (pWhiteWalker13) together with *plsY-gfp*. All pWhiteWalker plasmids were electroporated into RN4220 and used for FRET analysis.

### Whole genome sequencing

Integrity of *mreC* deficient strains was tested by whole genome sequencing. The by-product of unmarked deletions generation based on pIMAY chimeras results in two types of constructs: (i) successful unmarked deletions in the chromosome and (ii)

unsuccessful deletions resulting from plasmid excision from the chromosome and therefore ultimately resulting in a wild type genotype (the latter are here referred to as revertants). Two SH1000  $\Delta mreC$  and two reverted SH1000 wild type strains were sent for sequencing at the Sheffield Children'S NHS Trust Diagnostics Genetics Service (Sheffield, United Kingdom). Sequencing results can be found using the following link: <http://snurl.com/saureus> . The sequencing analysis revealed one amino acid substitution due to a single nucleotide polymorphism in each SH1000  $\Delta mreC$  compared to the revertants. One was found in gene SAOUHSC\_02282 encoding for the acetolactate synthase large subunit and one was found in gene SAOUHSC\_01710 encoding for the acetyl CoA carboxylase biotin carboxyl carrier protein.

### **Cell fractionation**

Membrane and cytoplasmic fractions of *S. aureus* strains were prepared as previously described with the following modifications. (6) Cells were resuspended in TBSi (50mM Tris, 100mM NaCl, pH=8, plus Complete Protease Inhibitor, Roche) to a density of 2500 OD<sub>600</sub> units/ml and cell breakage was undertaken with 0.1mm silica spheres (Lysing Matrix B, FastPrep Homogenizer; MP Biomedicals, Cambridge, UK). After two 25,000xg 10min centrifugation cycles to remove debris from the supernatant, a 171,500xg ultracentrifugation for 2h rendered cytoplasmic proteins in the supernatant while membranes resided in the pellet. The latter was subsequently resuspended in TBSi.

### **Antibodies**

Peptide 731 (LQVHADGPIS), was synthesized at the Core Facility at the University of Sheffield with an added C-terminal cysteine to enable conjugation to KLH or OVA carrier proteins. The KLH conjugate was used as an immunogen in rabbits to obtain polyclonal antibodies (BioServ, UK).

### **Protein immunoblot detection**

Proteins were separated and detected as previously described (11).

### **Fluorescence microscopy**

Epifluorescence microscopy preparations were made as previously described with the following modifications (12). Cells were resuspended in GTE buffer for mounting and the latter was performed using poly-L-lysine coated slides unless otherwise stated. For *in vivo* membrane stain, an aliquot from an exponentially growing culture was supplemented with Nile Red, FM4-64 or Nonyl-Acridine Orange at a final concentration of 1.25  $\mu\text{g ml}^{-1}$ , 0.12  $\mu\text{g ml}^{-1}$  and 0.47-2.36  $\mu\text{g ml}^{-1}$ , respectively. And then incubated for an additional 15min in the same conditions followed by washes with H<sub>2</sub>O and resuspension in GTE. Nile Red *in vitro* membrane stain of fixed samples was made at a concentration of 1.25  $\mu\text{g ml}^{-1}$ . Immunofluorescence preparations were undertaken as previously described (13) but lysostaphin treatment was applied at 1ng ml<sup>-1</sup>. The following goat anti-rabbit IgG secondary antibodies used were A-11008 Alexa Fluor 488-labelled to detect PlsY, and A-21071 Alexa Fluor 633-labelled antibodies to detect PlsY or MreD. For

peptidoglycan (cell wall) labeling, cells were grown according to the generic growth protocol indicated above. At an OD<sub>600</sub>~0.4-0.6 an aliquot of the culture received a vancomycin:vancomycin-AlexaFluor 594 solution (1:1; prepared as previously described (14)) to a final concentration of 1 $\mu$ g ml<sup>-1</sup>, and the culture was further incubated for an additional 15min in the same growth conditions. Then the cells were harvested, washed and processed as the epifluorescence samples indicated above. Cell enumeration and perimeter, major axis and minor axis measurements were performed using ImageJ 1.46o.

### **Electron microscopy**

Cultures of *S. aureus* for TEM processed as described previously (15) using 3% w/v Glutaraldehyde/0.1M Sodium Phosphate buffer as a fixative, a FEI Tecnai G2 Biotwin 120kv TEM (FEI UK Ltd, Cambridge, England) electron microscope and a Gatan MSC600CW High Sensitivity Fibre Coupled Camera. An adaptation of the TEM method was implemented for SEM, where hexamethyldisilazane (HEX) was used instead of propylene oxide and samples were then dried in a fume hood overnight before being placed onto SEM pin stubs, coated in gold and viewed in a Philips XL-20 Scanning Electron Microscope (Philips Ltd, Cambridge, England).

### **Flow cytometric analysis**

An assay culture of strain SH1000 *spa*- cells prepared as per the general growth conditions above and grown to an OD<sub>600</sub>~0.25 was centrifuged (5300xg 10min) and washed with PBS (3x) to be subsequently resuspended in PBS with half the original culture volume. A 100 $\mu$ l aliquot of this cell suspension was diluted 6-fold in reaction buffer (2% w/v BSA in PBS) to then receive 1 $\mu$ l of rabbit polyclonal anti-PlsY antibody ( $\alpha$ 731). The reaction was incubated on ice for 40 minutes on ice with periodic mixing by inversion. The primary antibody was removed by centrifugation (6900xg 30sec) followed by PBS washing (3x). The resulting cells were then resuspended in 1000 $\mu$ l of reaction buffer containing the labelled secondary antibody (Alexa Fluor488-conjugated Goat anti-rabbit IgG 2mg ml<sup>-1</sup>, Molecular Probes, UK) at a final dilution of 1:1000. Samples were incubated for 30 min at room temperature with gentle rocking. The samples were analyzed on a CyAnADP flow cytometer (Dako, Glostrup, Denmark). A minimum of 25,000 cells were collected for investigation. Analysis was undertaken using a 20-milliwatt, 488 nm solid state laser, cells were identified by light scatter (forward *versus* side) Immunofluorescence was measured using a 545 dichroic long pass and a 530/40 band pass filter. The data were analyzed using Summit 4.3 software (Dako).

### **Bacterial two-hybrid (BACTH) analyses**

$\beta$ -Galactosidase activity of BACTH strains was measured directly on solid media using the substrate X-Gal.  $\beta$ -Galactosidase hydrolyses X-Gal to produce  $\beta$ -D-galactopyranoside and 5-bromo-4-chloro-3-indolyl, the latter of which has a blue colouration and so is a visual indicator of  $\beta$ -galactosidase activity. To investigate interactions between MreD, PlsY and CdsA proteins, strains were grown overnight in 5 ml TSB amp (100), kan (50) at 37 °C, 250 rpm. The cell culture was sub-cultured in the same medium until the OD<sub>600</sub> ~0.5. Aliquots of 1 ml culture were harvested

by centrifugation at 13,200 rpm, 1 min and washed once by resuspension in 1 ml sterile Buffered LB and centrifugation. Cells were resuspended in 1 ml Buffered LB and a 100-fold dilution was made in sdH<sub>2</sub>O. 10 µl of this suspension was spotted onto freshly-made buffered LB agar plates containing 100 µg ml<sup>-1</sup> amp, 50 µg ml<sup>-1</sup> kan and 200 µg/ml X-Gal. Plates were incubated at 37°C for 12 hours followed by room temperature incubation for 36 hours.

### **Förster Resonance Energy Transfer (FRET) analyses**

FRET describes the transfer of excitation energy between two fluorophores without emission of a photon. This energy transfer is highly dependent on the distance between both fluorophores since the efficiency is inversely proportional to the sixth power of the distance between donor and acceptor. The FRET efficiency can be measured using donor photobleaching. The presence of an acceptor prevents the bleaching of the donor resulting in a longer decay time constant (16).

To investigate interactions between PlsY and the following membrane proteins, MreD, CdsA, SecY and MscL, strains were grown overnight in 5 ml BHI Ery(5)/Lin(25) at 37 °C, 250 rpm. The overnight culture was sub-cultured into fresh medium and incubated in similar conditions to early-exponential phase. This was used as inoculum for a subsequent culture in fresh medium supplemented with 1 mM IPTG and incubated at 37 °C, 250 rpm for 2 hours. Aliquots of 1 ml culture were harvested by centrifugation at 13,200 rpm, 1 min and washed once by resuspension in 1 ml PBS followed by fixing the cells in 4 % (w/v) para-formaldehyde at room temperature for 30 min, 90 rpm. Epifluorescence microscopy preparations were made as previously described. Photobleaching was carried out using a Nikon SMZ1500 stereomicroscope. GFP fluorescence was bleached over a time course of 5 min at a exposure time of 500 ms. Fluorescence intensity values were fitted and photobleaching decay time constants were calculated by CFP software (Beta v.1.0) using the formula  $y = \text{background} + \text{constant} * e^{-(\text{time}/\tau_{PB})}$ . The FRET efficiency was calculated using the following formula  $E = 1 - \tau'_{PB} / \tau_{PB}$  where  $\tau'_{PB}$  and  $\tau_{PB}$  are the photo-bleaching decay time constants of the donor in the absence and in the presence of the acceptor mCherry. In this study, expression of a tandem fusion of *plsY-gfp* was used as a control for FRET analysis for the absence of an acceptor. Statistical significance of FRET efficiency was calculated using a two-tailed two-sample Student's t-test.

## METHODS REFERENCES

1. Novick RP, Morse SI (1967) In vivo transmission of drug resistance factors between strains of *Staphylococcus aureus*. *J Exp Med* 125:45–59.
2. Schenk S, Laddaga RA (1992) Improved method for electroporation of *Staphylococcus aureus*. *FEMS Microbiol Lett* 73:133–138.
3. Sambrook J, Russell DW (2001) *Molecular Cloning: A Laboratory Manual* (CSHL Press).
4. Yu D, Sawitzke JA, Ellis H (2003) Recombineering with overlapping single-stranded DNA oligonucleotides: Testing a recombination intermediate. *P Natl Acad Sci USA* 100:7207.
5. Kreiswirth BN et al. (1983) The toxic shock syndrome exotoxin structural gene is not detectably transmitted by a prophage. *Nature* 305:709–712.
6. Cooper E, Garcia-Lara J, Foster S (2009) YsxC, an essential protein in *Staphylococcus aureus* crucial for ribosome assembly/stability. *BMC Microbiol* 9:266.
7. Novick RP (1991) Genetic systems in staphylococci. *Meth Enzymol* 204:587–636.
8. Arnaud M, Chastanet A, Debarbouille M (2004) New vector for efficient allelic replacement in naturally nontransformable, low-GC-content, Gram-Positive bacteria. *Appl Environ Microbiol* 70:6887–6891.
9. Monk IR, Shah IM, Xu M, Tan M-W, Foster TJ (2012) Transforming the untransformable: application of direct transformation to manipulate genetically *Staphylococcus aureus* and *Staphylococcus epidermidis*. *mBio* 3:1-11
10. Luong TT, Lee CY (2007) Improved single-copy integration vectors for *Staphylococcus aureus*. *J Microbiol Methods* 70(1):186-90.
11. Clarke SR, Harris LG, Richards RG, Foster SJ (2002) Analysis of Ebh, a 1.1-megadalton cell wall-associated fibronectin-binding protein of *Staphylococcus aureus*. *Infect Immun* 70:6680–6687.
12. Steele VR, Bottomley AL, Garcia-Lara J, Kasturiarachchi J, Foster SJ (2011) Multiple essential roles for EzrA in cell division of *Staphylococcus aureus*. *Mol Microbiol* 80:542–555.
13. Pinho MG, Errington J (2003) Dispersed mode of *Staphylococcus aureus* cell wall synthesis in the absence of the division machinery. *Mol Microbiol* 50:871–881.
14. Turner RD, Hurd AF, Cadby A, Hobbs JK, Foster SJ (2013) Cell wall elongation mode in Gram-negative bacteria is determined by peptidoglycan architecture. *Nature Commun* 4:1496.

15. Leatherbarrow AH, Yazdi MA, Curson JP, Moir A (1998) The *gerC* locus of *Bacillus subtilis*, required for menaquinone biosynthesis, is concerned only indirectly with spore germination. *Microbiol* 144:2125–2130.
16. Clegg R (2009) Förster resonance energy transfer – FRET: what is it, why do it and how it's done. In Gadella, Theodorus W. J. *FRET and FLIM Techniques. Laboratory Techniques in Biochemistry and Molecular Biology* 33:1–57.
17. Horsburgh MJ et al. (2002)  $\sigma^B$  modulates virulence determinant expression and stress resistance: characterization of a functional *rsbU* strain derived from *Staphylococcus aureus* 8325-4. *J Bacteriol* 184:5457–5467.
18. Bottomley, AL (2011) Identification & characterisation of the cell division machinery of *Staphylococcus aureus*. PhD thesis. University of Sheffield (Sheffield, United Kingdom)
19. Zuberi AR, Moir A, Feavers IM (1987) The nucleotide sequence and gene organization of the *gerA* spore germination operon of *Bacillus subtilis* 168. *Gene* 51:1–11.
20. Karimova G, Dautin N, Ladant D (2005) Interaction network among *Escherichia coli* membrane proteins involved in cell division as revealed by bacterial two-hybrid analysis. *J Bacteriol* 187:2233–2243.
21. Jana M, Luong T-T, Komatsuzawa H, Shigeta M, Lee CY (2000) A method for demonstrating gene essentiality in *Staphylococcus aureus*. *Plasmid* 44:100–104.
22. Kaltwasser M, Wiegert T, Schumann W (2002) Construction and application of epitope- and green fluorescent protein-tagging integration vectors for *Bacillus subtilis*. *Appl Environ Microbiol* 68:2624–2628.
23. Horsburgh MJ et al. (2002) MntR modulates expression of the PerR regulon and superoxide resistance in *Staphylococcus aureus* through control of manganese uptake. *Mol Microbiol* 44:1269–1286.
24. Brosius J (1989) Superpolylinkers in cloning and expression vectors. *DNA* 8:759–777.
25. Krogh A, Larsson B, von Heijne G, Sonnhammer EL. (2001) Predicting transmembrane protein topology with a hidden markov model: application to complete genomes. *J Mol Biol* 305:567–580.
26. Spyropoulos IC, Liakopoulos TD, Bagos PG, Hamodrakas SJ (2004) TMRPres2D: high quality visual representation of transmembrane protein models. *Bioinformatics* 20:3258–3260.
27. Russ JC (2007) *The Image Processing Handbook* (CRC Press).

## SUPPLEMENTARY TABLES

**Supplementary Table 1. Bacterial strains**

Strain	Features	Source
<i>Staphylococcus aureus</i> strain		
SH1000 parental background		
JGL153	Tet-P <sub>spac</sub> ~ <i>plsY</i> <sup>+</sup>	This study
JGL166	JGL153 pGL485 Tet <sup>R</sup> Cat <sup>R</sup>	This study
JGL227	P <sub>ezrA</sub> : <i>ezrA</i> ~GFP+ P <sub>spac</sub> : <i>ezrA</i> +	(12)
JGL229	P <sub>mreC</sub> : <i>mreC</i> ~GFP+ P <sub>spac</sub> : <i>mreC</i> +	This study
JGL230	P <sub>mreD</sub> : <i>mreD</i> ~GFP+ P <sub>spac</sub> : <i>mreD</i> +	This study
JGL231	P <sub>secY</sub> : <i>secY</i> ~GFP+ P <sub>spac</sub> : <i>secY</i> +	This study
JGL232	P <sub>plsY</sub> : <i>plsY</i> ~GFP+ P <sub>spac</sub> : <i>plsY</i> +	This study
JGL233	P <sub>ezrA</sub> : <i>ezrA</i> ~GFP+ P <sub>spac</sub> : <i>ezrA</i> + P <sub>spac</sub> : <i>plsY</i> + pGL485	(12)
JGL234	P <sub>mreC</sub> : <i>mreC</i> ~GFP+ P <sub>spac</sub> : <i>mreC</i> + P <sub>spac</sub> : <i>plsY</i> + pGL485	This study
JGL236	P <sub>mreD</sub> : <i>mreD</i> ~GFP+ P <sub>spac</sub> : <i>mreD</i> + P <sub>spac</sub> : <i>plsY</i> + pGL485	This study
JGL240	P <sub>secY</sub> : <i>secY</i> ~GFP+ P <sub>spac</sub> : <i>secY</i> + P <sub>spac</sub> : <i>plsY</i> + pGL485	This study
JGL241	JGL166 P <sub>xyl</sub> -Pbp2~gfp	This study
JGL260	P <sub>plsY</sub> : <i>plsY</i> ~GFP+ P <sub>spac</sub> : <i>plsY</i> + pGL485	This study
LC102	SH1000 spa-	(6)
SH1000	8325-4 <i>rsbU</i> <sup>+</sup>	(17)
SH1000 / pGL484	P <sub>plsY</sub> : <i>plsY</i> + P <sub>spac</sub> ~ <i>plsY</i> +	This study
SJF2625	<i>mreCD</i> :: <i>kan</i>	This study
SJF2976	<i>mreD</i> :: <i>kan</i>	This study
SJF4098	$\Delta$ <i>mreC</i>	This study
SJF4650	<i>mreD</i> :: <i>kan</i> <i>lip</i> ::P <sub>mreCD</sub> : <i>mreD</i>	This study
SJF4651	<i>lip</i> ::P <sub>mreCD</sub> : <i>mreD</i>	This study
RN4220 parental background		
JGL145	pGL484	This study
JGL219	P <sub>plsY</sub> : <i>plsY</i> ~GFP+ P <sub>spac</sub> : <i>plsY</i> +	This study
JGL223	P <sub>mreC</sub> : <i>mreC</i> ~GFP+ P <sub>spac</sub> : <i>mreC</i>	This study
JGL224	P <sub>mreD</sub> : <i>mreD</i> ~GFP+ P <sub>spac</sub> : <i>mreD</i>	This study
JGL225	P <sub>secY</sub> : <i>secY</i> ~GFP+ P <sub>spac</sub> : <i>secY</i>	This study
SJF4057	RN4220 pXIM5	This study
RNpBP2-31	P <sub>xyl</sub> -Pbp2~gfp	(13)

**Supplementary Table 2.** Plasmids used in this manuscript

Plasmids	Relevant markers and genotype	Origin
pALB11	pUT18C containing T18 fused in frame to the 5' end of <i>S. aureus mreD</i> ; Amp <sup>R</sup>	(18)
pALB7	pKT25 containing T25 fused in frame to the 5' end of <i>S. aureus mreD</i> ; Kan <sup>R</sup>	(18)
pAZ106	Promoterless <i>lacZ erm</i> insertion vector	(19)
pGL400	Tet-T-P <sub>spac</sub> cassette containing vector	(6)
pGL401	pOB derivative containing a region of <i>plsY</i> from <i>S. aureus</i> SH1000	This study
pGL412	derivative of pGL401 containing Tet-T-P <sub>spac</sub> ~ <i>plsY</i>	This study
pGL433	Kan <sup>R</sup> cassette containing plasmid	(6)
pGL456	reduced size pAZ106 derivative with a deletion that encompasses <i>lacZ</i> and containing the MCS from pSL1190	This study
pGL471b	<i>S. aureus</i> stable pGL456 derivative containing the pE194 temperature sensitive origin of replication (pE194ts)	This study
pGL484	pGL471b derivative rrnTet5 P <sub>pen</sub> -rbs <i>lacI cat</i> (pC194) ori(pE194) Tet <sup>R</sup> (pT181) ori(pGB2) Spc <sup>R</sup> (pGB2) Tet-T-P <sub>spac</sub> ~ <i>plsY</i>	This study
pGL485	<i>lacI</i> pE194ori Cat <sup>R</sup> ( <i>S. aureus</i> ) Spec <sup>R</sup> ( <i>E. coli</i> )	(6)
pGL503	pMutinGFP+ containing <i>S. aureus plsY</i> at the KpnI/EagI sites	This study
pGL516	pMutinGFP+ containing <i>S. aureus mreC</i> at the KpnI/EagI sites	This study
pGL517	pMutinGFP+ containing <i>S. aureus mreD</i> at the KpnI/EagI sites	This study
pGL519	pMutinGFP+ containing <i>S. aureus secY</i> at the KpnI/EagI sites	This study
pGL555	pKT25 containing T25 fused in frame at the BamHI/EcoRI sites to the 5' end of <i>S. aureus plsY</i> ; Kan <sup>R</sup>	This study
pGL568	pUT18C containing T18 fused in frame at the BamHI/EcoRI sites to the 5' end of <i>S. aureus plsY</i> ; Amp <sup>R</sup>	This study
pGL589	pOb derivative containing the 5' (~2.2kb) and 3' (~1kb) flanking regions of <i>mreD</i> from the <i>S. aureus</i> chromosome	This study
pGL607a	pGL589 derivative containing a Kan <sup>R</sup> cassette (from pGL433) in between the <i>mreD</i> flanking regions	This study



pGL613	pMAD derivative containing the <i>mreD</i> upstream-Kan <sup>R</sup> - <i>mreD</i> downstream region from pGL607a	This study
pGL633	pKT25 containing T25 fused in frame at the EcoRI/BamHI sites to the 5' end of <i>S. aureus cdsA</i> Kan <sup>R</sup>	This study
pGL635	pUT18 containing T18 fused in frame at the EcoRI/BamHI sites to the 3' end of <i>S. aureus cdsA</i> ; Amp <sup>R</sup>	This study
pKNT25	derivative of low copy-number pSU40, carrying gene encoding the first 224 amino acids of CyaA (T25 fragment), downstream of a multiple cloning site; Kan <sup>R</sup>	(20)
pKT25	Derivative of low copy-number pSU40, carrying the first 224 amino acids of <i>B.subtilis</i> CyaA (T25 fragment), upstream of a multiple cloning site; Kan <sup>R</sup>	(20)
pKT25- zip	pKT25 containing T25 fused in frame to the 5' end of the leucine zipper of GC84; Kan <sup>R</sup>	(20)
pLL2443	pE194ts origin of replication flanked by ClaI sites	(21)
pMAD	<i>E. coli</i> - <i>S. aureus</i> shuttle vector with temperature-sensitive replication origin in <i>S. aureus</i> and constitutively expressed thermostable $\beta$ -galactosidase gene	(8)
pMUTIN-GFP+	GFP+ containing vector	(22)
pOB	Cloning vector containing <i>erm</i> resistance gene	(23)
pSL1190	DNA polyliner containing 64 uninterrupted hexameric recognition sites	(24)
pUT18	Derivative of high copy-number pUC19, carrying gene encoding amino acids 225 to 399 of CyaA (T18 fragment), downstream of a multiple cloning site; Amp <sup>R</sup>	(20)
pUT18C	Derivative of high copy-number pUC19, carrying gene encoding amino acids 225 to 399 of CyaA (T18 fragment), upstream of a multiple cloning site; Amp <sup>R</sup>	(20)
pUT18C- zip	pUT18C containing T18 fused in frame to the 5' end of the leucine zipper of GC84; Amp <sup>R</sup>	(20)
pWhiteWalker0	<i>E.coli</i> - <i>S.aureus</i> shuttle vector similar to pGL471b but containing the origins of replication pT181 (instead of pE194ts) and pMB1 P <sub>pen</sub> -rbs <i>lacI</i> T-P <sub>spac</sub> Ery <sup>R</sup> ( <i>S. aureus</i> ) Amp <sup>R</sup> ( <i>E. coli</i> )	This study
pWhiteWalker1	<i>E.coli</i> - <i>S.aureus</i> shuttle vector with IPTG-inducible expression of <i>mCherry</i> and <i>gfp</i> ; Ery <sup>R</sup> ( <i>S. aureus</i> ) Amp <sup>R</sup> ( <i>E. coli</i> )	This study

pWhiteWalker2	<i>E.coli-S.aureus</i> shuttle vector with IPTG-inducible expression of <i>mCherry-gfp</i> ; Ery <sup>R</sup> ( <i>S. aureus</i> ) Amp <sup>R</sup> ( <i>E. coli</i> )	This study
pWhiteWalker3	<i>E.coli-S.aureus</i> shuttle vector with IPTG-inducible expression of <i>mreD-mCherry</i> and <i>plsY-gfp</i> ; Ery <sup>R</sup> ( <i>S. aureus</i> ) Amp <sup>R</sup> ( <i>E. coli</i> )	This study
pWhiteWalker4	<i>E.coli-S.aureus</i> shuttle vector with IPTG-inducible expression of <i>cdsA-mCherry</i> and <i>plsY-gfp</i> ; Ery <sup>R</sup> ( <i>S. aureus</i> ) Amp <sup>R</sup> ( <i>E. coli</i> )	This study
pWhiteWalker10	<i>E.coli-S.aureus</i> shuttle vector with IPTG-inducible expression of <i>plsY-gfp</i> ; Ery <sup>R</sup> ( <i>S. aureus</i> ) Amp <sup>R</sup> ( <i>E. coli</i> )	This study
pWhiteWalker12	<i>E.coli-S.aureus</i> shuttle vector with IPTG-inducible expression of <i>secY-mCherry</i> and <i>plsY-gfp</i> ; Ery <sup>R</sup> ( <i>S. aureus</i> ) Amp <sup>R</sup> ( <i>E. coli</i> )	This study
pWhiteWalker12	<i>E.coli-S.aureus</i> shuttle vector with IPTG-inducible expression of <i>secY-mCherry</i> and <i>plsY-gfp</i> ; Ery <sup>R</sup> ( <i>S. aureus</i> ) Amp <sup>R</sup> ( <i>E. coli</i> )	This study
pCL25	Amp <sup>R</sup> <i>E. coli</i> replicating plasmid (non-replicating in <i>S.aureus</i> ) for ectopic gene integration in the lipase gene of <i>S. aureus</i> using Tet <sup>R</sup> as an integration marker	(10)
pCL25- <i>mreD</i>	pCL25 derivative containing <i>mreD</i> under the control of its native promoter	This study
pYL112Δ19	Expression of integrase, required for integration of pCL25, Cm <sup>R</sup> ( <i>S.aureus</i> )	(10)

---

**Supplementary Table 3. Oligonucleotides used in this study**

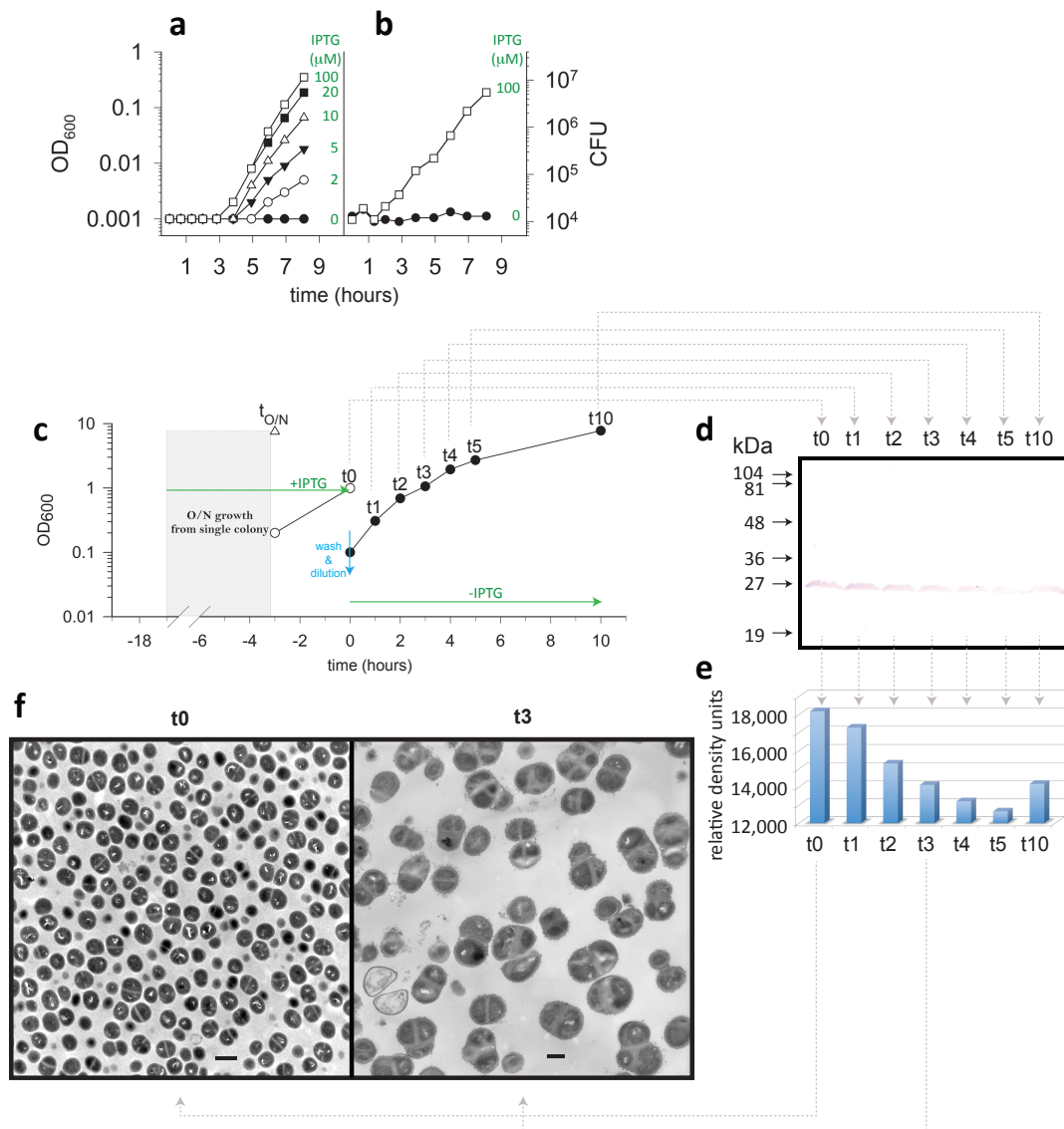
Oligonucleotide name	Oligonucleotide sequence (5' – 3') <sup>(1)</sup>	Construction of :
3'GLUSh302Q	ATAATAGAA <u>TTCTT</u> ACATCCATTTTATTTTAGGTTTC	pGL568, pGL555
3'GLUSh406A	ATAATAGAA <u>TTCTT</u> AGATTGTATTAATAAAATATTTAA TAATG	pGL635, pGL633
3'GLUSh16c	tagtaacatgacgattatcatcataaatattacacatc cttAATTGTGAGCGGCTCACAATTCCAC	pGL412
3' GLUSh66a	aaccggttccatgtgctcgccgagggcggcataaatcgc cgtgacgATGATTACGCCAAGCTTAAG	pGL456
3'GLUSh190A	ATTATACGGCCGCATCCATTTTATTTTAGGTTTC	pGL503
3'GLUSh270A	ATATTTGGTACCGTCAGCACGTTTAG	pGL613 pGL589 pXIM5
3'GLUSh270B	ATATTTGCGGCCGCTACTTATAACTACTCAACTATTG	Kan <sup>R</sup> (6)
5'GLUSh27B	ATTTGCGGCCGCGATAAACCCAGCGAACCATTTG	
3'GLUSh27B	ATTTGGCCGGCCATCGATACAAATTCCTCGTAG	
3'GLUSh270C	ATAAATGCGGCCGCTACATACAACCGCTCAAATATAGG TTC	pGL589
3'GLUSh270D	AATTATGCGGCCGCAAAAAATAATACAGTGTACG	pGL589
3'GLUSh3f	ATAAGGATCCGTTTCTGGGTTCATCGTCGT	pGL484
3'GLUSh3K	gaccgagcgcagcgcagtcagtgagcgcaggaagcggaag agcTCTGGGTTCATCGTCGTTTC	pGL401
3'HXM39B	ATAATAGCGGCCGCATCGATACAAATTCCTCG	pGL607a
3'HXM67A	ATATTTAGATCTGTGACGACGTTTAG	pGL613
3'JCK31D	ATAATACGGCCGTTTATCCCTGCTTTCATCA	pGL516
3'JCK31E	ATAATACGGCCGCCATTGACGACGTTTCATG	pGL517
3'JCK31G	ATAATACGGCCGCTCTACCACCAAAGCCTTTA	pGL519
5'GLUSh302Q	ATAATAGGATCCTATGATGATAATCGTCATGTTAC	pGL568, pGL555
5'GLUSh406A	ATAATAGGATCCAATGAAAGTTAGAACGCTG	pGL635, pGL633
5'GLUSh16c	agccgtaattttaaatgaatatgataaaatagtcctaag atattaAGAAATCCCTTTGAGAATGTTT	pGL412
5'GLUSh190A	ATTATAGGTACCAGGAGGTGTAATATTTATG	pGL503
5'GLUSh270A	ATATTTGGATCCTAATGTGGAAGTAG	pGL589
5'GLUSh270B	ATATTTGCGGCCGCCACAAATTTTTTACGGAG	pXIM5
5'GLUSh270C	AATATTGCGGCCGCTCTATTATGTCAAATATTG	
5'GLUSh270D	ATTATGCGGCCGCTAAAACAATTCCTGATGATG	
5'GLUSh3f	ATAAGGATCCAAGCGGTTATGCTGAAACT	pGL484
5'GLUSh3K	aataccgcacagatgcgtaaggagaaaaataccgcatca ggaAAGCGGTTATGCTGAAACT	pGL401
5'GLUSh66a	atcagttgctgttgactgtagcggctgatgttgaaactg gaagtcgTGAATTCGAATGGCCATGGG	pGL456
5'HXM292	ATAATAGAGCTCCTAATGTGGAAGTAG	pXIM5

5'HXM39B	ATAATAGCGGCCGCATAAACCCAGCGAACCATTTG	pGL607a
5'JCK31D	ATAATAGGTACCTAGAGGTGTTCTGGGTGC	pGL516
5'JCK31E	ATAATAGGTACCAGCAGGGATAAATAATGCG	pGL517
5'JCK31G	ATAATAGGTACCACGAGGTGATCTAATGATTCA	pGL519
5'FL04	AAAGAATTCAGGAGGATAAAACACATGGGCGTTAGTAA AGGCG	pWhiteWalker1,2,3,4
3'FL04OE	aagttcttctcctttactcatGGATCCACCAGAACCag atcttttatataattcatcc	pWhiteWalker2
5'FL05OE	ggatgaattatataaaAAGATCTGGTTCTGGTGGATCCa tgagtaaaggagaagaac	pWhiteWalker2
3'FL05	AAAGGCGCGCCCTATTTGTATAGTTCATCCA	pWhiteWalker1,2
5'FL06	TTTAGATCTTGATTAGGAGGATGAACCGGTATGATGAT AATCGTCATG	pWhiteWalker5
3'FL06	AAAGGTACCCGAGCCCGAGCCCATCCATTTTATTTTAG G	pWhiteWalker5
5'FL07	TTTGAATTCTTAGGAGGAAATTATTGAATGCGTACACT GTAT	pWhiteWalker3
3'FL07OE	tcttcgcctttactaacgcccattGCTGCCGCTGCCGCT AGcccattgacgacgttt	pWhiteWalker3
5'FL08OE	aaacgtcgtcaatggGCTAGCGGCAGCGGCAGCatggg cgttagtaaaggcgaaga	pWhiteWalker3
5'FL09	TTTGAATTCTTAGGAGGATGAAATTATATGAAAGTTAG AACG	pWhiteWalker4
3'FL09OE	tcttcgcctttactaacgcccattGCTGCCGCTGCCGCT AGCagattgtattaataaaaatattt	pWhiteWalker4
5'FL10OE	aaatattttattaataacaatctGCTAGCGGCAGCGGCA GCatgggcgtagtaaaggcgaaga	pWhiteWalker4
3'pWhiteWalker 0mCherryOE	aagttcttctcctttactcatGGTACCTCATCCTCCTA ATCAagatcttttatataattcatcc	pWhiteWalker1
5'pWhiteWalker 0GFPOE	ggatgaattatataaaagatctTGATTAGGAGGATGAG GTACCatgagtaaaggagaagaac	pWhiteWalker1
5'FW73	CAATTAAGCTTGATATCGAGGAGGATGAACCGGTATG	pWhiteWalker10
3'FW73	ATTATGCATTTAGAATAGGGGCGCGCCCTATTTGTAT	pWhiteWalker10
5'FW75	CAATTAAGCTTGATATCGGAATTCTTAGGAGGAAATTA TTGAATGATTCAAACCCTTGTGAAC	pWhiteWalker12
3'FW75	ATGCTGCCGCTGCCGCCTCTACCACCAAAGCCTTTATA TTC	pWhiteWalker12
5'FW76	CAATTAAGCTTGATATCGGAATTCTTAGGAGGAAATTA TTGAATGTTAAAAGAATTCAAAGAGTTTCG	pWhiteWalker13
3'FW76	ATGCTGCCGCTGCCGCCTTTTTTCTCACGTAATAAATC TCTG	pWhiteWalker13
5'FW94	CCTTTTTTTTGCCCCGGTTTTAACTACTAGTGACTGGAA TG	pCL25-mreD

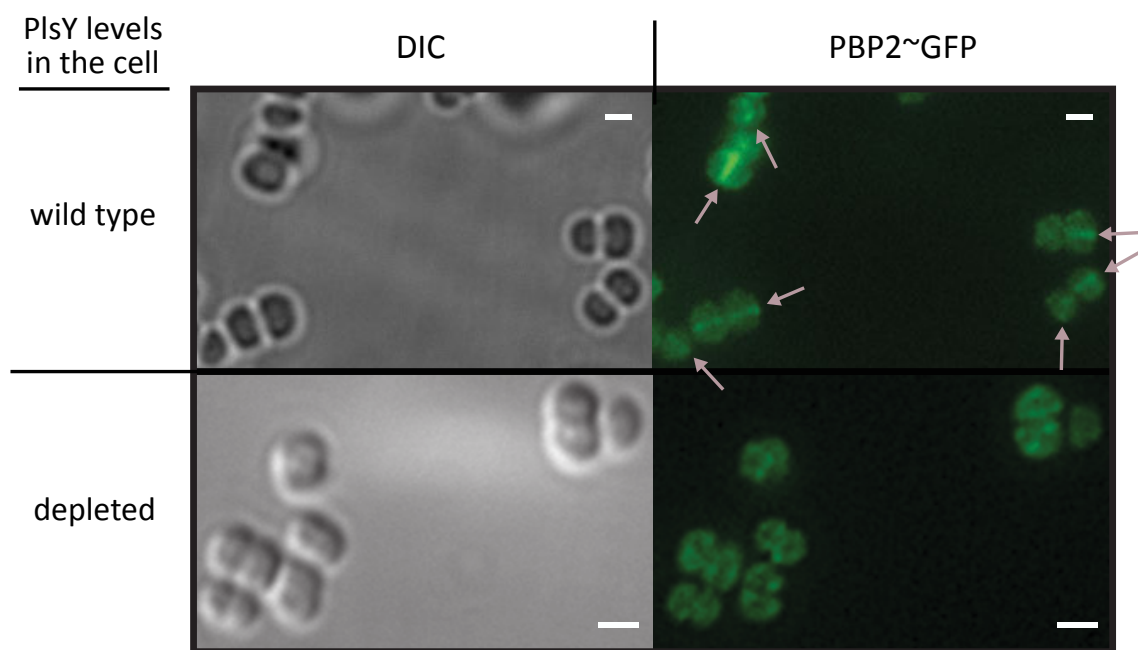
3'FW94	CTGCTTTCTTGTATATCCTTTTCTATTTTATATTACTC C	pCL25-mreD
5'FW95	GGATATACAAGAAAGCAGGGATAAATAATGC	pCL25-mreD
3'FW93	CTATGACCATGATTACGTTACCATTGACGACGTTTC	pCL25-mreD

---

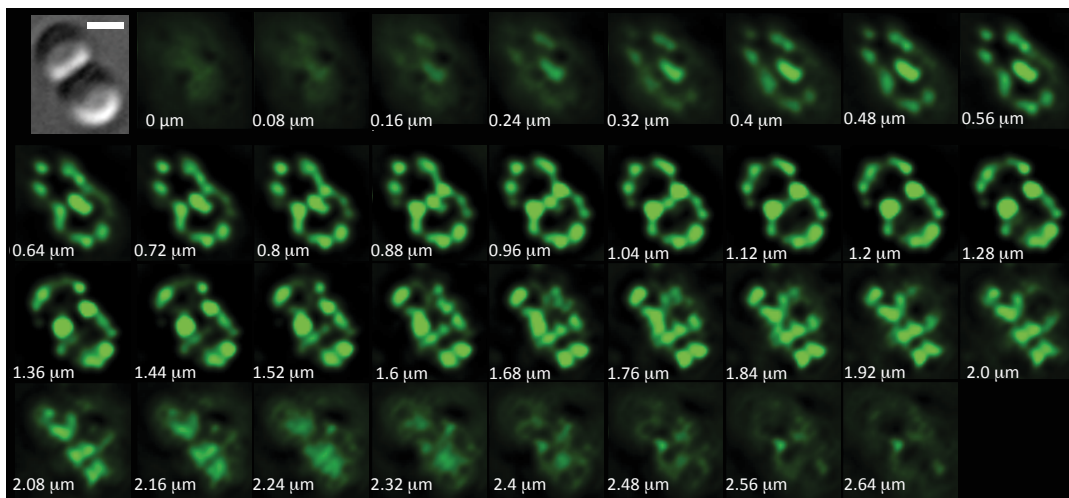
<sup>(1)</sup> Lower case, sequences for Lambda Red cloning and overlap extension PCR; underlined, engineered restriction sites.



**Supplementary Fig. 1**, PlsY is an essential protein in *S. aureus*. Growth of strain *S. aureus* JGL166, which contains a single copy of *plsY* under the control of the regulatable P<sub>spac</sub> promoter, depends on the presence of the exogenous inducer (IPTG) in a dose dependent manner, as determined by spectrophotometric absorbance –OD<sub>600</sub>– (**a**) or viable counts (**b**). (**c**) Following growth in the presence of the exogenous inducer (t<sub>0/N</sub> and t<sub>0</sub>), its subsequent removal results in an impairment of growth correlated with the disappearance of PlsY in the cells (t<sub>0</sub>-t<sub>10</sub>) as determined by Western blot immunodetection using polyclonal antibody α-731 on whole cell extracts at various timepoints during growth (**d**), and quantitated through the determination of pixel density for each band with ImageJ 1.46o (**e**). (**f**) TEM images of the morphological aberrations of cells deprived of PlsY after 3 hours of growth in the absence of IPTG (t<sub>3</sub>) compared to the wild type appearance of the culture at t<sub>0</sub> (immediately after IPTG removal). Scale bars, 1 μm

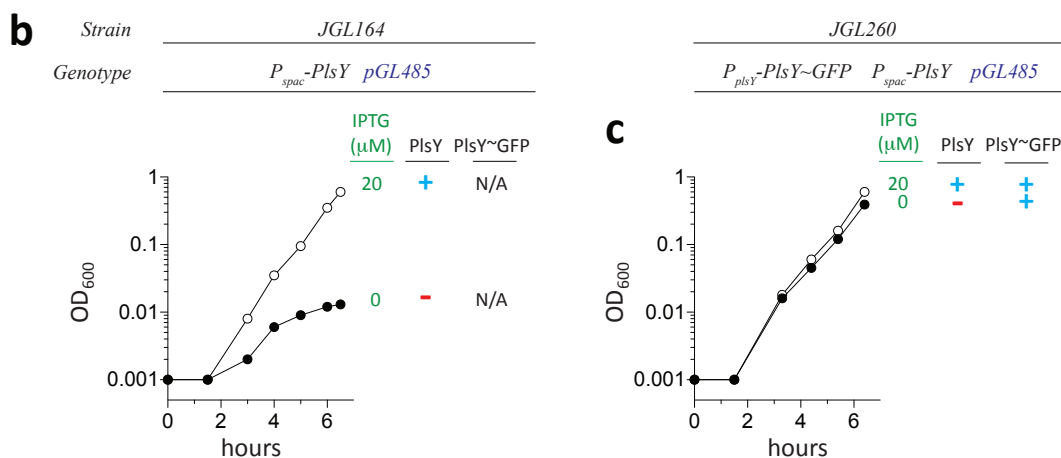
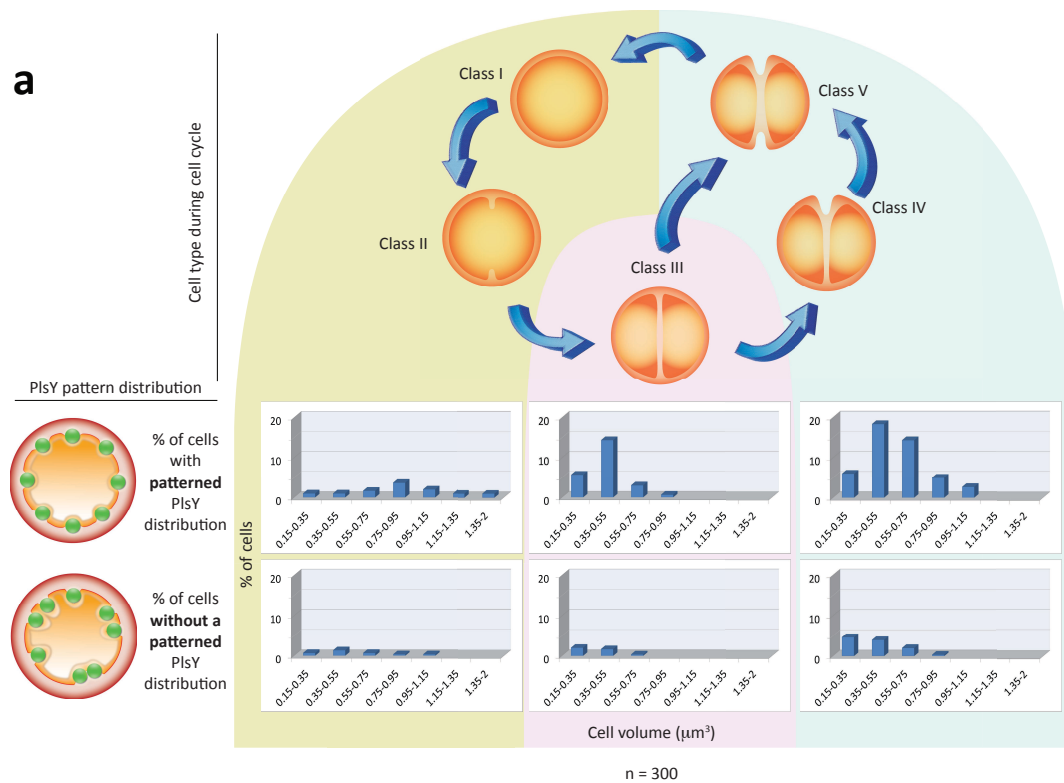


**Supplementary Fig. 2,** Pbp2~GFP which localizes at mid-cell in wild type cells during division (arrows) is abnormally distributed in PlsY depleted cells. Scale bars, 1 $\mu$ m

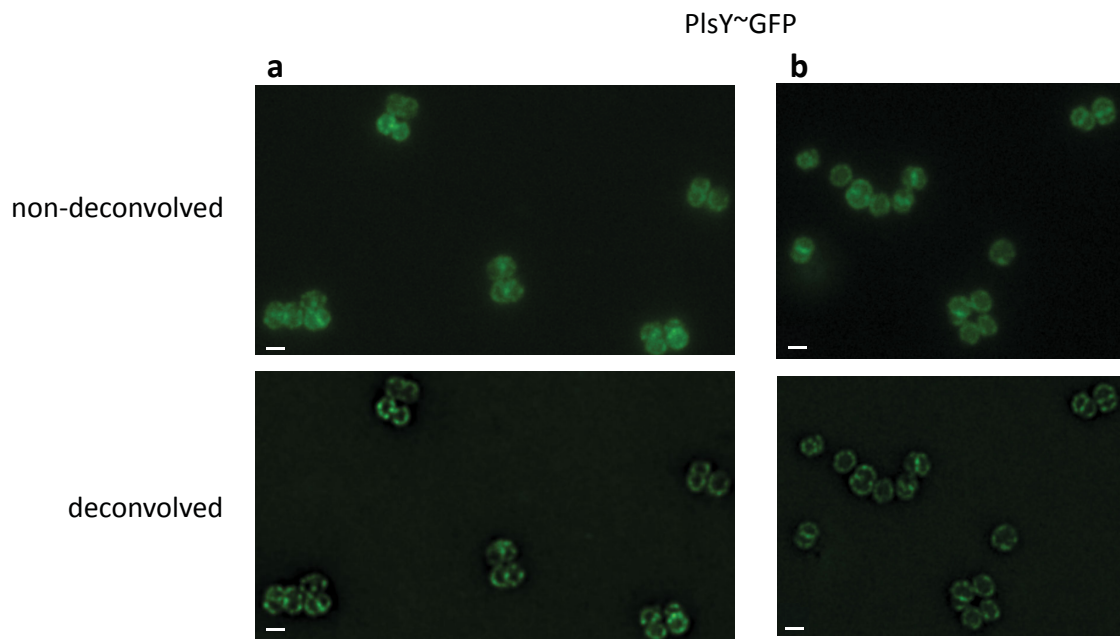


**Supplementary Fig. 3,** Optical dissection through the Z-axis of a PlsY~GFP in *S. aureus* reveals a PlsY network in the *S. aureus* membrane. Scale bars, 1  $\mu\text{m}$

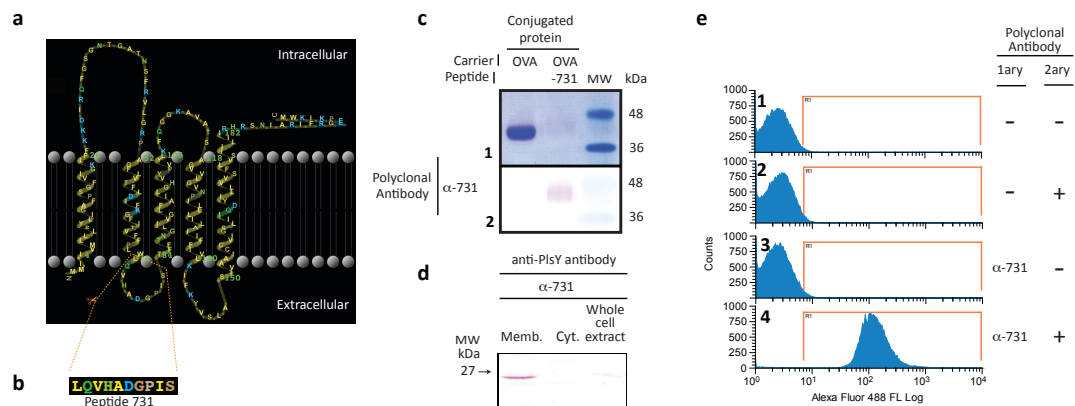




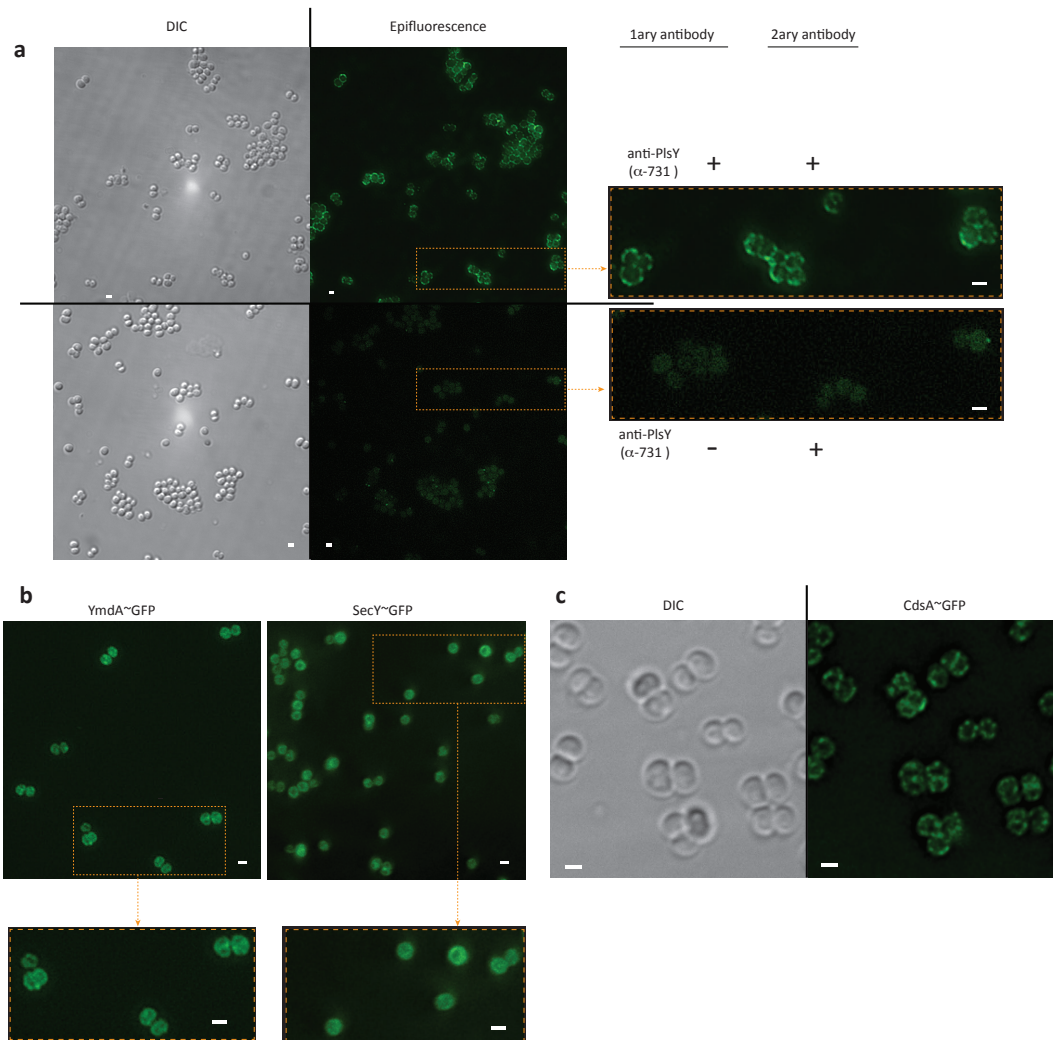
**Supplementary Fig. 4a**, Frequency of cells within the population exhibiting regular and non-regular distribution of PlsY~GFP within the membrane at the various stages of the cell cycle (n= 300); **b**, Complementation of growth deficiency due to PlsY depletion (growth of  $P_{spac}$ ~*plsY* in the absence of the IPTG inducer) (**b**), by the PlsY-GFP fusion expressed from the *plsY* native promoter (in strain JGL260) (**c**).



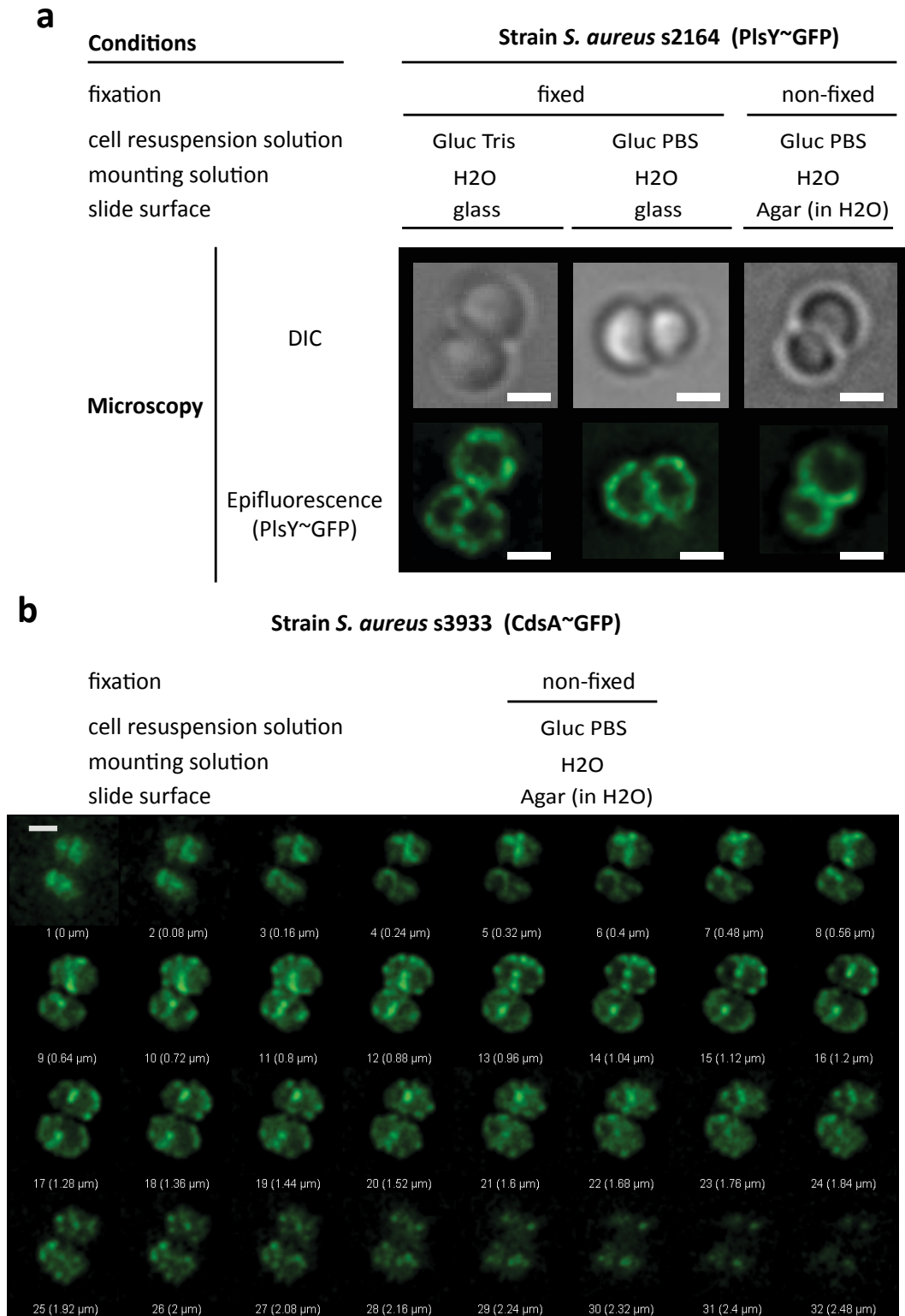
**Supplementary Fig. 5**, Two different microscopy fields (**a**, **b**) illustrating the patterned distribution of PlsY~GFP in the *S. aureus* JGL232 membrane, which can be distinguished in non-deconvolved and deconvolved forms of the same image, albeit the latter allows for sharper discrimination. Scale bars, 1  $\mu$ m.



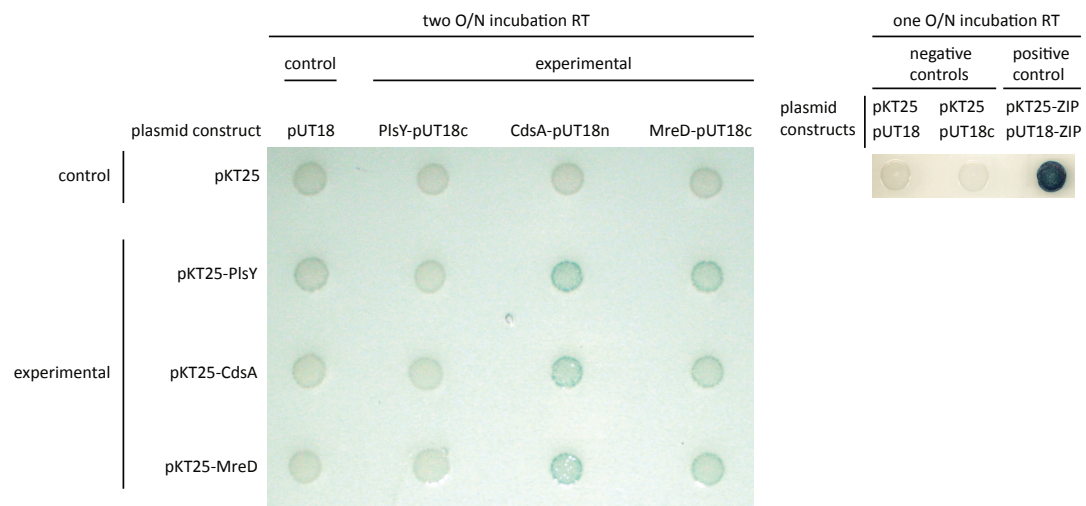
**Supplementary Fig. 6a**, Transmembrane topology prediction of PlsY calculated by the TMHMM method and visually represented using TMRPres2D. (24, 25) **b**, peptide sequence 731 of the predicted extramembranous loop of PlsY was used as antigen through NHS coupling to carrier protein KLH for the production of rabbit polyclonal antibody  $\alpha$ -731. **c**,  $\alpha$ -731 polyclonal sera specifically detects (Western Blot) its cognate peptide conjugated to ovalbumin (OVA) without cross-reactivity. A purified preparation of ovalbumin (OVA) or OVA-conjugated 731 peptide were challenged with anti-731 sera. **d**, PlsY is a membrane protein in *S. aureus*, as determined by Western Blot in protein extracts of *S. aureus* cellular compartments (membrane, cytoplasm and whole cell extracts) with  $\alpha$ -731. Cellular extracts were obtained from a *spa*- strain containing a single wild type *plsY* gene (LC102). **e**, FACS-mediated detection of PlsY in live cells of *S. aureus* LC102 (*spa*-) with  $\alpha$ -731 (primary antibody sources, 1ary) and goat anti-rabbit Alexa Fluor 488 (fluorescently labelled secondary antibody).



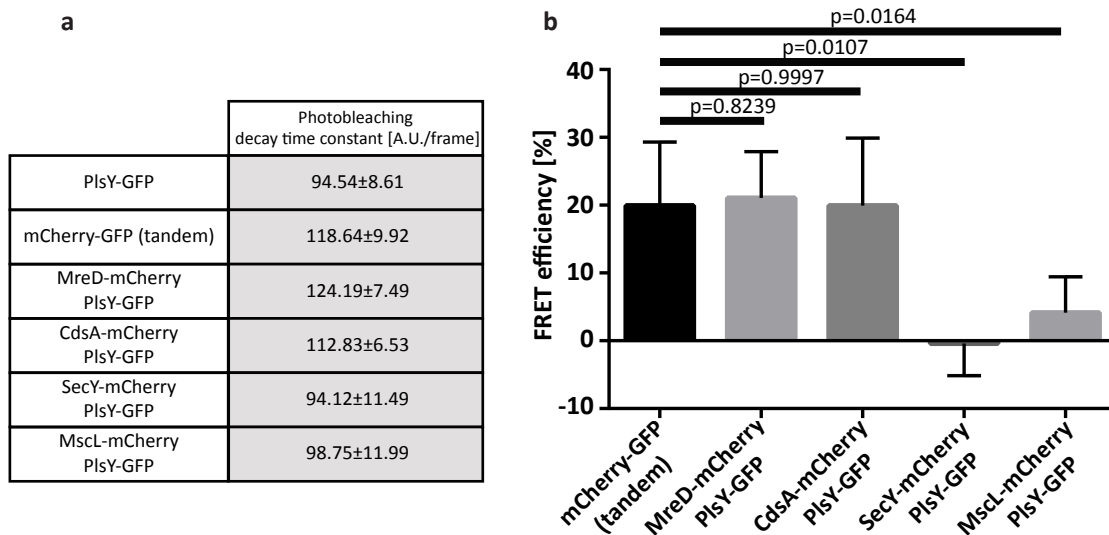
**Supplementary Fig. 7a**,  $\alpha$ -731-mediated immunolocalization of PlsY in *S. aureus* LC102 (*spa*-); **b**, Other GFP-tagged membrane proteins, YmdA and SecY have a diffused distribution pattern in *S. aureus* SH1000; **c**, distribution of CdsA~GFP in *S. aureus* SH1000.



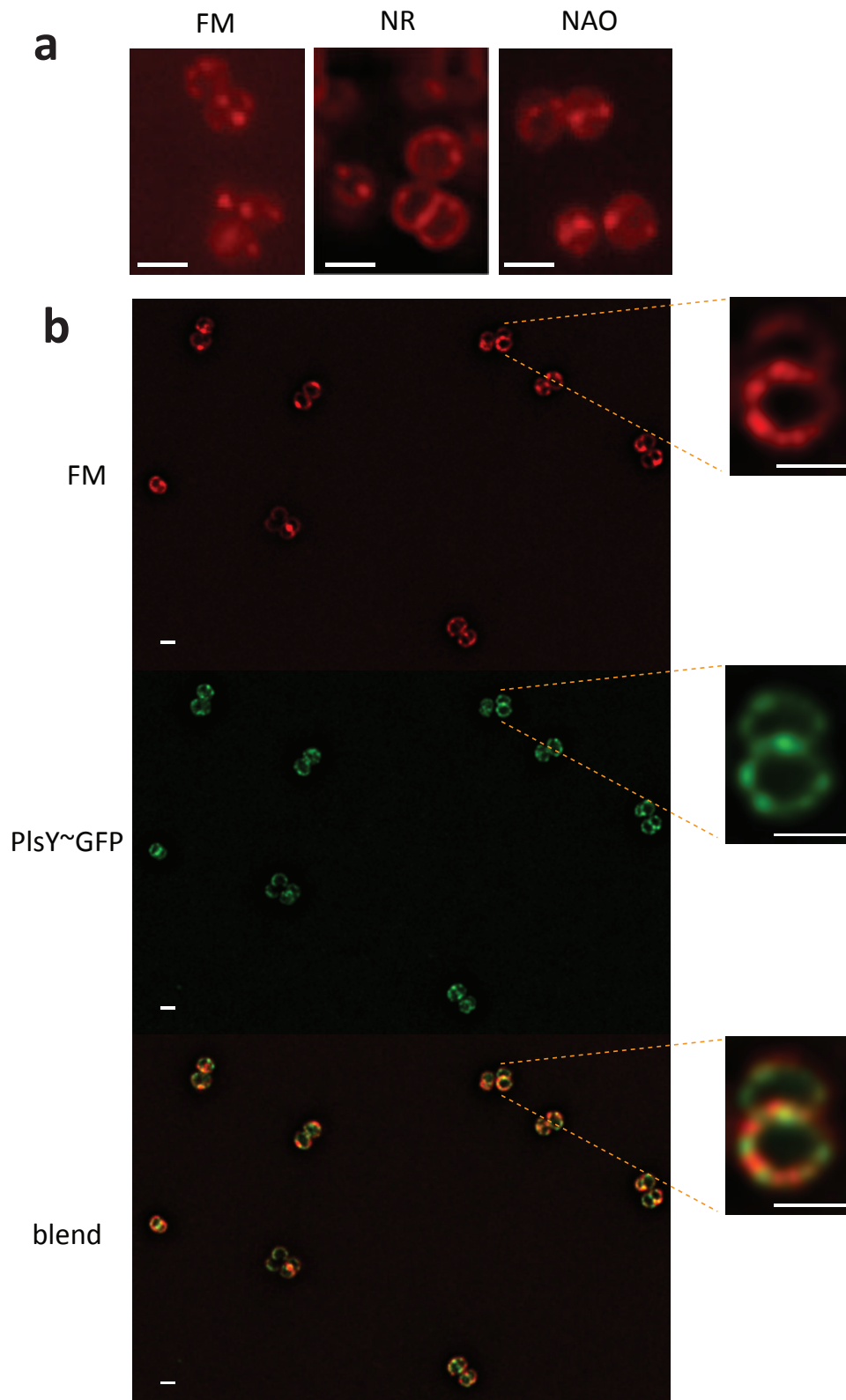
**Supplementary Fig. 8**, Distribution pattern of GFP-tagged PlsY(**a**) and CdsA(**b**) in the membrane of non-fixed cells mounted in H<sub>2</sub>O or 1% w/v Agar in H<sub>2</sub>O. Scale bars, 1 μm.



**Supplementary Fig. 9**, Protein-protein interactions shown by BACTH analyses.

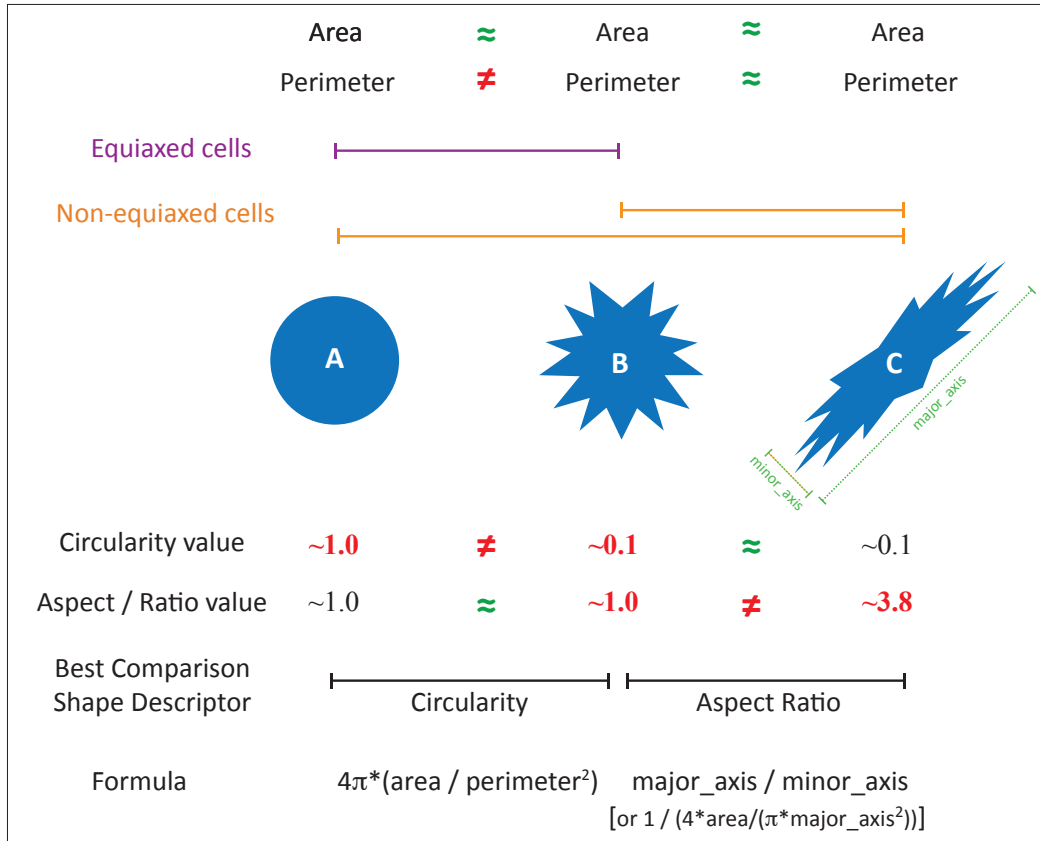


**Supplementary Fig. 10**, Protein-protein interactions shown by FRET analyses between a PlsY-GFP and other membrane proteins tagged with mCherry. **a**, Photobleaching decay time constants. **b**, FRET efficiencies of mCherry membrane protein fusions compared to the of PlsY-GFP fusion alone. The mCherry membrane protein fusions encompass an mCherry-GFP protein tandem fusion which acts as a positive control, and the MreD, CdsA, SecY and MscL membrane proteins. FRET analyses shows the interaction of PlsY with CdsA and MreD but not with another two membrane proteins, SecY or MscL.

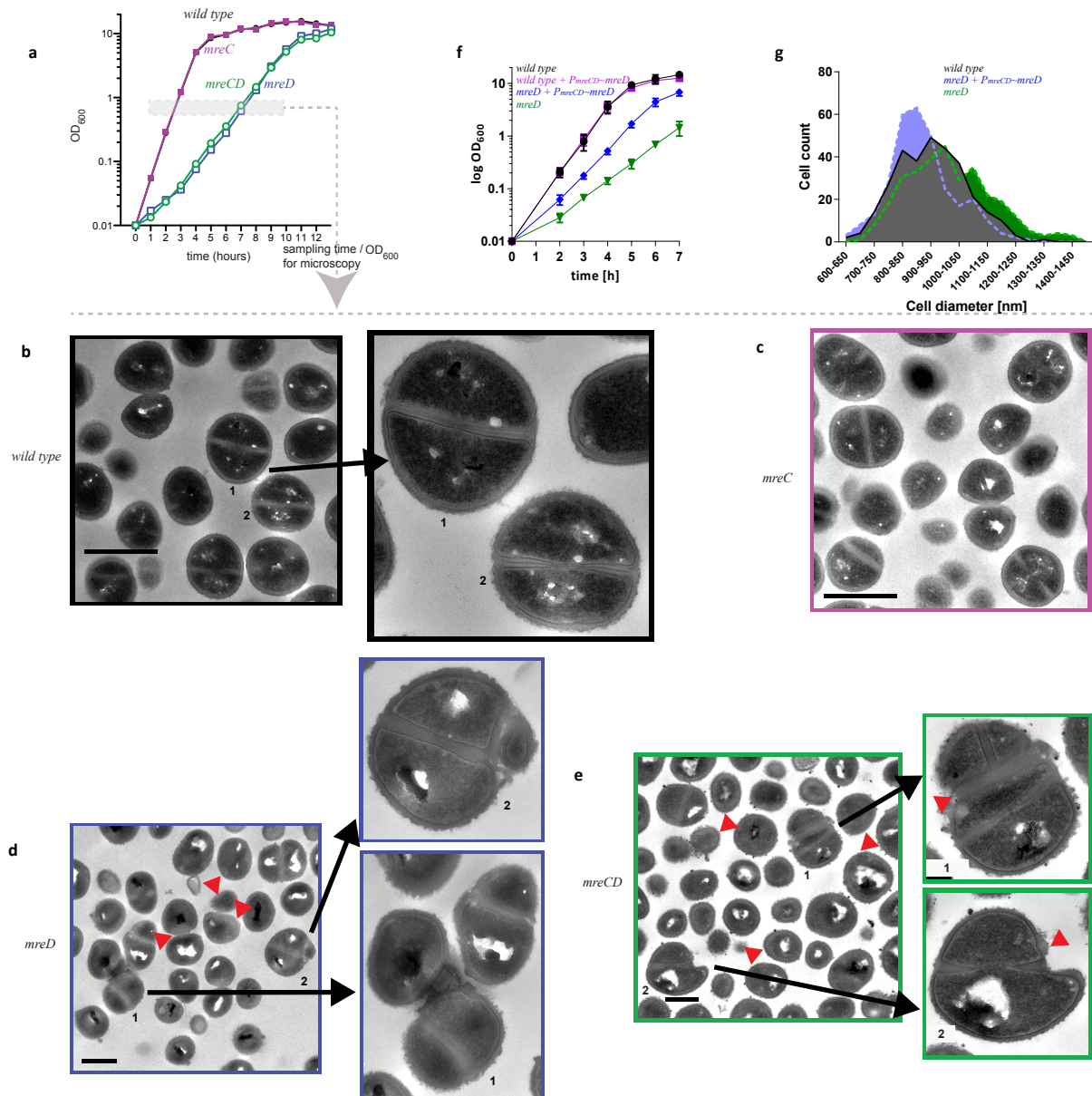


**Supplementary Fig. 11.a**, Clustered distribution of lipids in the membrane of live *S. aureus* as revealed by the neutral lipid stain Nile Red (NR) and the generic lipid stain FM4-64 (FM) in epifluorescence microscopy. Nonyl-Acridine Orange (NAO) only stains anionic phospholipids, which show high concentration at the septa. **b**, distribution of lipids (stained with FM4-64) and PlsY~GFP in the membrane of *S. aureus* JGL232. Scale bars, 1µm.

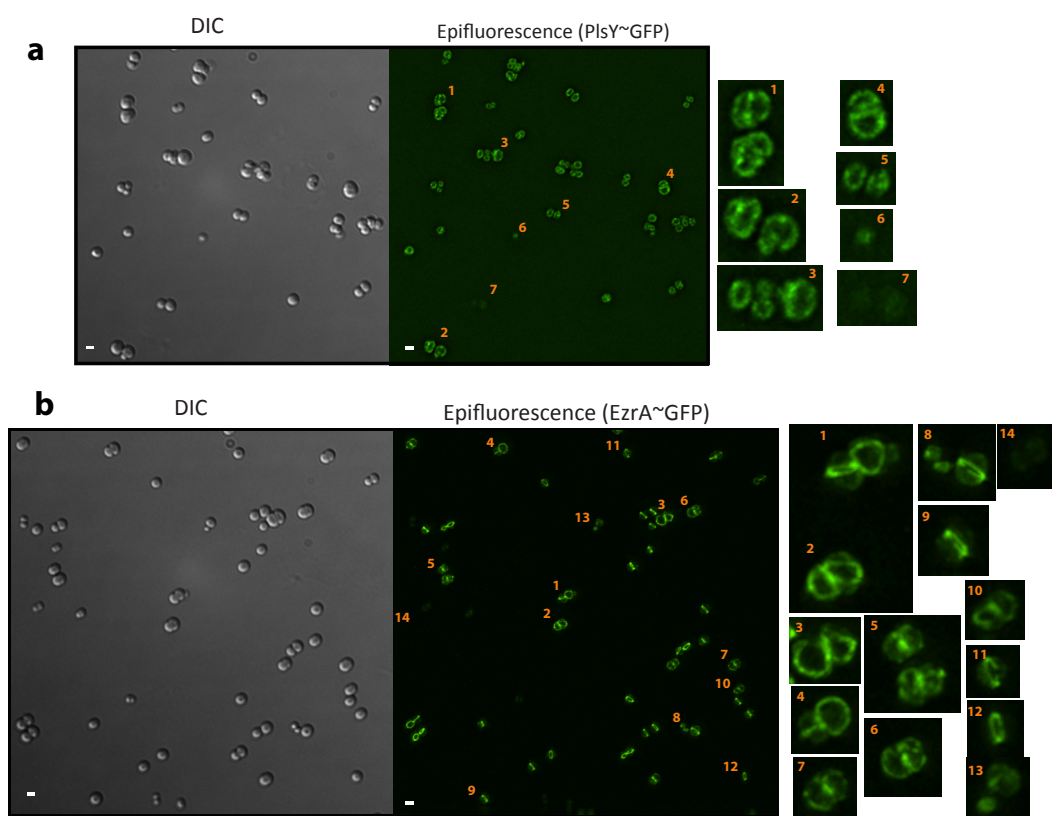




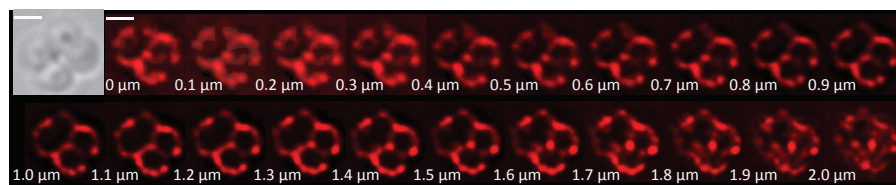
**Supplementary Fig. 12**, Explanation on cell shape descriptors used in this manuscript based on that previously described (26). The evaluation of shape abnormalities due to *mreD* deficiency in Fig. 3 is undertaken through two dimensionless ratios: i) **Cell Circularity**, -x axis of the graphs- compares the area of a cell to its perimeter using the formula  $4\pi \times (\text{area} / \text{perimeter}^2)$ ; and, ii) **Cell Aspect Ratio (AR)**, -illustrated by the width of the symbol- compares the ratio between the longest and the shortest axis of the cell ( $\text{major\_axis} / \text{minor\_axis}$ ; or the inverse of  $4 \times \text{area} / (\pi \times \text{major\_axis}^2)$ ) (26). The larger the width the more elongated the cell or cell cluster. An ideal circle would have a value of 1.0 for both, Circularity and AR; and this would be the average value for single cells of wild type *S. aureus*. Cells that develop irregular boundaries would have a Circularity  $< 1.0$  while those that become elongated would result in  $\text{AR} > 1$ . The different shape of approximately equiaxed cells is better described by the Circularity parameter (compare A and B). However, for non-equiaxed cells (compare C with A or B) irregularity is better described by their AR.



**Supplementary Fig. 13.a**, Growth time of *S. aureus* SH1000 wild type (●, black), *mreC* deletion mutant (strain SJF4098; ■, pink), *mreD* deletion mutant (strain SJF2976; □, blue), and *mreCD* deletion mutant (strain SJF2625; ○, green) for TEM (**b**, **c**, **d** and **e**) examination of cellular morphology; **f**, the growth impairment of *mreCD* deficient *S. aureus* (strain SJF2625) can be complemented by a single-copy of *mreD* driven by the upstream *mreCD* promoter region that was ectopically integrated at the lipase gene in the chromosome of the *mreD* deletion mutant; it complemented the *mreD* deficient growth (**f**) and cell morphology (**g**) phenotypes.



**Supplementary Fig. 14**, Effect of MreD deficiency on PlsY (a) and EzrA (b) distribution. Scale bars, 1  $\mu\text{m}$ .



**Supplementary Fig. 15**, Optical dissection through the Z-axis of immunolocalized MreD in *S. aureus* reveals a MreD network in the *S. aureus* similar to the PlsY network. Scale bars, 1 $\mu$ m.

**Supplementary Fig. 16, Theoretical mathematical modelling of pattern formation by protein complexes embedded in the membrane.**

As discussed in the text, we start with the free energy

$$\mathcal{F} = \frac{\kappa}{2} \int dA [H^2 - 2H_p \rho a_0 H] + \frac{1}{2\chi} \int dA [\xi^2 (\nabla \psi)^2 + \psi^2] + \frac{kR^2}{2} \int dA u^2. \quad (1)$$

We can extract the effective force that is exerted on the membrane in the radial direction and use it together with the friction force in a force balance equation that describes the shape of the membrane

$$\partial_t u(\theta, \phi, t) = -L_u \frac{\delta \mathcal{F}}{\delta u(\theta, \phi)}, \quad (2)$$

where  $L_u$  is the membrane mobility (a transport coefficient). The dynamical equation describing the diffusion of the protein complexes can be written as a continuity equation

$$\partial_t \psi(\theta, \phi, t) + \nabla \cdot \mathbf{J} = 0, \quad (3)$$

where the current density is given as  $\mathbf{J} = -L_\psi \nabla \mu$  in terms of the chemical potential

$$\mu = \delta \mathcal{F} / \delta \psi(\theta, \phi), \quad (4)$$

with  $L_\psi$  being another transport coefficient. Putting these together, we find the equation that governs the diffusion of the protein complex as

$$\partial_t \psi(\theta, \phi, t) = -L_\psi \nabla^2 \left( \frac{\delta \mathcal{F}}{\delta \psi(\theta, \phi)} \right). \quad (5)$$

On the spherical surface, the Laplacian operator is in the form of  $\nabla^2 = -\frac{1}{R^2} \hat{L}^2$ , where

$$-\hat{L}^2 = \frac{1}{\sin \theta} \partial_\theta (\sin \theta \partial_\theta) + \frac{1}{\sin^2 \theta} \partial_\phi^2, \quad (6)$$

which is diagonal in the basis of spherical harmonics  $Y_{\ell m}(\theta, \phi)$ , namely

$$\hat{L}^2 Y_{\ell m}(\theta, \phi) = \ell(\ell + 1) Y_{\ell m}(\theta, \phi). \quad (7)$$

Using this, we can write Eqs. (2) and (5) as

$$\partial_t u(\theta, \phi, t) = -L_u \left[ \frac{\kappa}{R^2} \hat{L}^2 (\hat{L}^2 - 2) u + \frac{\kappa H_p a_0 \rho_0}{R} (\hat{L}^2 + 2) \psi + kR^2 u \right], \quad (8)$$

$$\partial_t \psi(\theta, \phi, t) = -\frac{L_\psi}{R^2} \left[ \frac{1}{\chi} \hat{L}^2 \psi + \frac{1}{\chi} \left( \frac{\xi^2}{R^2} \right) \hat{L}^4 \psi + \frac{\kappa H_p a_0 \rho_0}{R} \hat{L}^2 (\hat{L}^2 - 2) u \right], \quad (9)$$

to the leading order.

We can write

$$u(\theta, \phi, t) = \sum_{\ell, m} u_{\ell m}(t) Y_{\ell m}(\theta, \phi), \quad (10)$$

and

$$\psi(\theta, \phi, t) = \sum_{\ell, m} \psi_{\ell m}(t) Y_{\ell m}(\theta, \phi) \quad (11)$$

and rewrite the dynamical equations (8) and (9) for the amplitudes of the different modes. Using a rescaled time variable

$$\tau = \left( \frac{\kappa L_u}{R^2} \right) t, \quad (12)$$

and the dimensionless parameters

$$K = kR^4 / \kappa, \quad (13)$$

$$S = \rho_0 a_0 H_p R, \quad (14)$$

$$M = L_\psi / (\kappa L_u \chi), \quad (15)$$

$$B = \kappa \chi / R^2, \quad (16)$$

$$P = \xi^2 / R^2, \quad (17)$$

we find

$$-\dot{u}_{\ell m} = [\ell(\ell+1)(\ell+2)(\ell-1) + K] u_{\ell m} + S [\ell(\ell+1) + 2] \psi_{\ell m}, \quad (18)$$

$$-\frac{1}{M} \dot{\psi}_{\ell m} = [\ell(\ell+1) + P\ell^2(\ell+1)^2] \psi_{\ell m} + BS [\ell(\ell+1)(\ell+2)(\ell-1)] u_{\ell m}, \quad (19)$$

where  $\dot{x} \equiv \partial_\tau x$ . Putting in

$$u_{\ell m}(\tau) = u_{\ell m}(0) e^{\lambda\tau}, \quad (20)$$

$$\psi_{\ell m}(t) = \psi_{\ell m}(0) e^{\lambda\tau}, \quad (21)$$

we can find an equation for the growth rates corresponding to the characteristic modes of the system by setting the determinant of the coefficients to zero. This reads

$$[\lambda + \ell(\ell+1)(\ell+2)(\ell-1) + K] \left[ \frac{\lambda}{M} + \ell(\ell+1) + P\ell^2(\ell+1)^2 \right] - W\ell(\ell+1)(\ell+2)(\ell-1) [\ell(\ell+1) + 2] = 0, \quad (22)$$

where

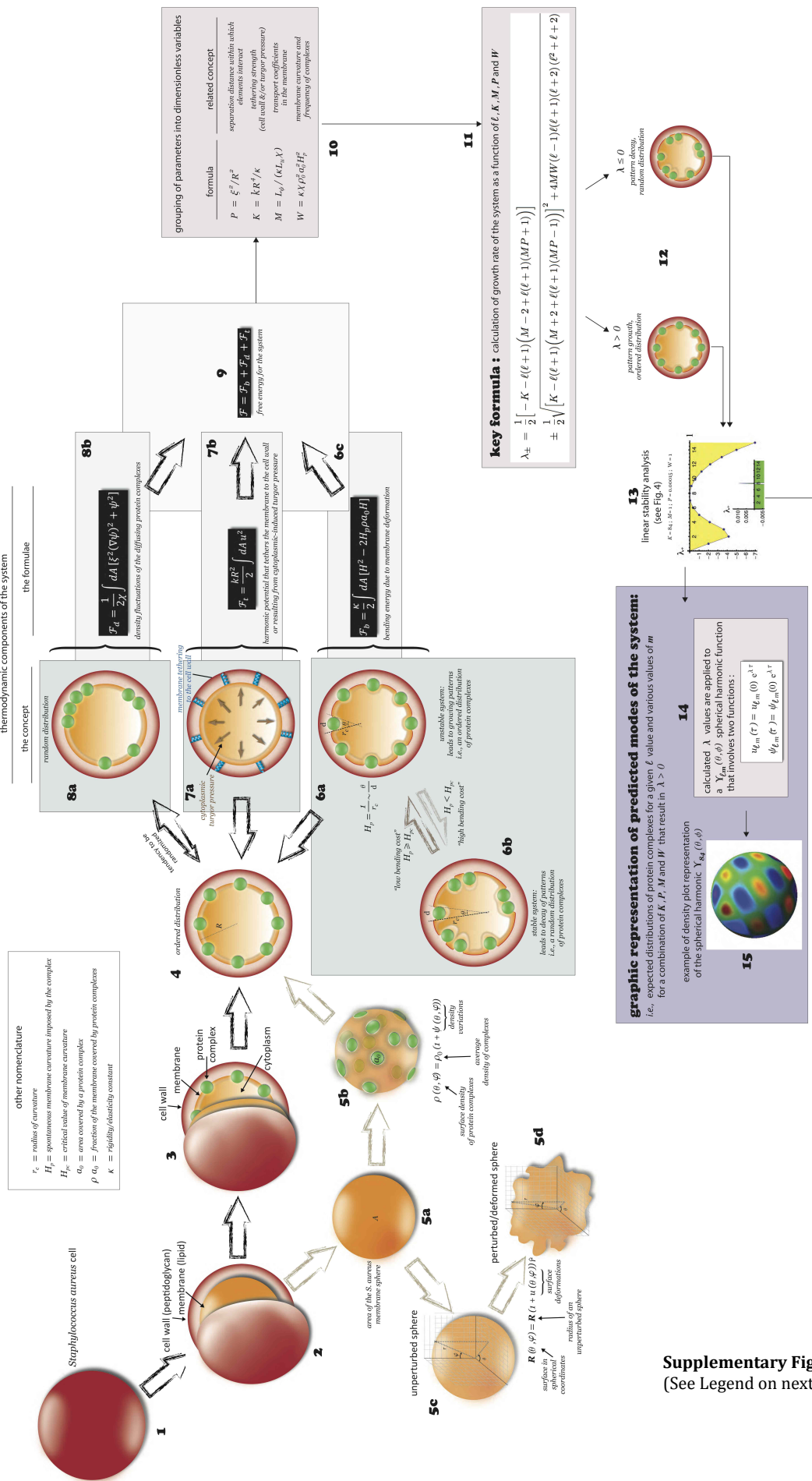
$$W \equiv BS^2 = \kappa\chi\rho_0^2 a_0^2 H_p^2. \quad (23)$$

Solving Eq. (22) gives the two rates  $\lambda_+$  and  $\lambda_-$  as

$$\begin{aligned} \lambda_{\pm} = & \frac{1}{2} \left[ -K - \ell(\ell+1) \left( M - 2 + \ell(\ell+1)(MP+1) \right) \right] \\ & \pm \frac{1}{2} \sqrt{\left[ K - \ell(\ell+1) \left( M + 2 + \ell(\ell+1)(MP-1) \right) \right]^2 + 4MW(\ell-1)\ell(\ell+1)(\ell+2)(\ell^2 + \ell + 2)}. \end{aligned} \quad (24)$$

We note that  $\lambda_-$  is always negative, and hence, the corresponding mode is always stable. However,  $\lambda_+$  could become positive at selected intermediate  $\ell$  values, and lead to an instability with a certain pattern.  $\lambda_+$  from Eq. (24) is plotted in Fig. 4 for  $K = 84$ ,  $M = 1$ ,  $P = 0.00015$ , and different values of  $W$  near 1, along with the spherical harmonics corresponding to the example with  $\ell = 8$ .

Our results are robust with respect to the numerical choices for our parameters. Choosing values in the range  $30 < K < 180$  and  $0.1 < M < 10$  would lead to an intermediate wavevector unstable mode with the  $\ell$ -index in the range of 6–10, with the threshold value of the only sensitive or tuning parameter, namely  $W$ , remaining near 1. Our choice of  $P = 0.00015$  corresponds to a correlation length of order  $\xi \simeq 12$  nm (using  $R \simeq 1 \mu\text{m}$ ), which is a reasonable estimate for the distance at which protein clusters sense the presence of neighboring clusters via elastic interactions. We expect  $M$  to be of order 1 because it reflects competition between two (appropriately compared) friction coefficients in the same system. While it is hard to estimate  $k$ , our choice of  $K \simeq 100$  appears reasonable; it corresponds to a stiffness that leads to an elastic energy cost that is two orders of magnitude larger than the bending energy cost for the membrane when strongly deformed.



**Supplementary Fig. 17**  
(See Legend on next page)

**key finding :** (see also Supplementary Fig. 12)  
 $W$  - the dimensionless variable greatly dependent on the local curvature of the cell membrane imposed by a protein/complex, is the most sensitive of all parameters determining the distribution of proteins/complexes in the membrane. While minimal changes in  $W$  result in values of  $\lambda \approx 0$ , therefore leading to decay or random distribution of protein patterns in the membrane, significant variations on the values of  $K$ ,  $P$ , or  $M$  are required to attain the same outcome. Hence, proteins and protein complexes will tend to group or cluster in a manner that they impose only thermodynamically favourable bending costs in the membrane ultimately resulting in their uniform or patterned distribution in the membrane.

**Supplementary Fig. 17**, The distribution of proteins and protein complexes in the bacterial membrane is a three-dimensional phenomenon that can be defined by an unknown mathematical function that depends on multiple independent variables. To ascertain the solution to the partial differential equation describing the generation or dispersal of protein patterns in the membrane and the relation between the various variables, the first step is to identify the system and the variables that define it. In this case, our system consists of the virtually spherical *Staphylococcus aureus* cell (1) –in principle, the simplest bacterial shape-, composed of an outermost peptidoglycan-based cell wall (2) enclosing a lipidic membrane, within which we have observed embedded proteins and/or protein complexes distributed in a regular pattern (3, a cartoon of a transverse section of a *S. aureus* cell; and 4, a cartoon corresponding to the microscopic plane of focus at midcell). Primary variables in our system are the area of the cell membrane ( $A$ , defined here as an unperturbed sphere in its radial form; 5a,c), the area covered by a protein complex ( $a_0$ ; 5b), and the density of the complexes ( $\rho$ ; 5b). 5d, illustrates the case of a deformed sphere. The presence of a protein complex within the membrane is bound to induce a membrane deformation in the latter that can be factored into the equation by defining the surface through its spherical coordinates (6a,b). The resulting membrane curvature ( $H_p$ ) will entail a bending cost, which will depend on the elasticity/rigidity constant of the membrane ( $\kappa$ ). If the curvature is larger than a critical threshold ( $H_{pc}$ ) it will result in a system, which would be considered as unstable (from a physics standpoint, but stable biologically) i.e., it will enable the growth of patterns. If  $H_p < H_{pc}$  the resulting system will lead to the decay of patterns. These variables and constants describe part of the energy of the system, specifically the energy resulting from membrane deformation ( $\mathcal{F}_b$ ; 6c). Another contribution comes from the forces that tether the membrane to the surrounding cell wall, or the cytoplasmic turgor pressure (7a), which are dependent on a spring constant ( $k$ ), and are represented mathematically as  $\mathcal{F}_t$ . (7b) The final contribution originates from the entropy of the mixing of the proteins/complexes as they are distributed in the membrane and their fluctuations (8a), which is denoted as  $\mathcal{F}_d$  (7c). The free energy of the overall system ( $\mathcal{F}$ ), which does not change in its components but in its properties, is therefore the combined result of  $\mathcal{F}_b + \mathcal{F}_d + \mathcal{F}_t$  (9). The dynamical equations, which describe the time evolution of the system, would allow us to study the growth or decay of the protein patterns in the membrane (10). For convenience when solving the corresponding differential equations, the parameters are grouped as dimensionless variables. Interestingly, although these variables do not directly correspond to easily distinguishable biological variables, it is possible to elucidate how they relate to them in terms of controlling the relative competition between the energy contributions: where  $\mathbf{K}$  relates to  $\mathcal{F}_t$  versus  $\mathcal{F}_b$  (tethering),  $\mathbf{P}$  and  $\mathbf{M}$  relate to  $\mathcal{F}_d$  (transport coefficients, i.e., physicochemical properties of lipids and proteins) and  $\mathbf{W}$  relates to  $\mathcal{F}_d$  versus  $\mathcal{F}_b$  (membrane curvature due to presence of protein complexes). The solutions to the equation are two functions  $\lambda_+$  and  $\lambda_-$ , representing the growth or decay of protein patterns in the membrane (11). The condition of equilibrium of the system, or a stable system in physics leading to a random protein complex distribution in the membrane would correspond to  $\lambda = 0$  (no protein pattern formation) (12). As  $\lambda_-$  is never positive it will always lead to



random/uniform distribution of proteins without protein pattern formation. In contrast, some values and combination of values for  $K$ ,  $P$ ,  $M$  and  $W$  as a function of the characteristic modes of the system (**1**) may result in positive  $\lambda$  + (See Fig. 4 and Supplementary Figs. 12 and 13). The representation of growth rates as a function of each characteristic mode results in a linear stability analysis (**13**), while the separation of variables into spherical coordinates leads to spherical harmonics of the form  $(Y_{lm}(\theta, \varphi))$  (**14**) that can be represented as a density plot (**15**).